

Adipose recruitment and activation of plasmacytoid dendritic cells fuel metaflammation

**Amrit Raj Ghosh¹, Roopkatha Bhattacharya¹, Shamik Bhattacharya¹, Titli Nargis²,
Oindrila Rahaman¹, Pritam Duttagupta¹, Deblina Raychaudhuri¹, Chinky Shiu Chen Liu¹,
Shounak Roy¹, Parasar Ghosh³, Shashi Khanna⁴, Tamonas Chaudhuri⁴, Om Tantia⁴,
Stefan Haak⁵, Santu Bandyopadhyay¹, Satinath Mukhopadhyay⁶, Partha Chakrabarti² and
Dipyaman Ganguly^{1*}.**

Divisions of ¹Cancer Biology & Inflammatory Disorders and ²Cell Biology & Physiology, CSIR-
Indian Institute of Chemical Biology, Kolkata, India;

⁴ILS Hospitals, Kolkata, India;

⁵Zentrum Allergie & Umwelt (ZAUM), Technical University of Munich and Helmholtz Centre
Munich, Munich, Germany;

Departments of ³Rheumatology and ⁶Endocrinology, Institute of Postgraduate Medical Education
& Research, Kolkata, India.

*Corresponding author:

Dipyaman Ganguly,

Division of Cancer Biology & Inflammatory Disorders,

CSIR-Indian Institute of Chemical Biology,

4 Raja S C Mullick Road, Jadavpur, Kolkata, West Bengal, India, 700032.

Phone: 91 33 24730492 Fax: 91 33 2473 5197

Email: dipyaman@iicb.res.in

Running title: PDCs and type I interferons in metaflammation

Word count (Main text): 5521 Figures: 7, Table: 1

ABSTRACT

In obese individuals the visceral adipose tissue (VAT) becomes seat of chronic low grade inflammation (metaflammation). But the mechanistic link between increased adiposity and metaflammation remains largely unclear. We report here that in obese individuals deregulation of a specific adipokine, chemerin, contributes to innate initiation of metaflammation, by recruiting circulating plasmacytoid dendritic cells (pDCs) into visceral adipose tissue via chemokine-like receptor 1 (CMKLR1). Adipose tissue-derived high mobility group B1 (HMGB1) protein, activates toll-like receptor 9 (TLR9) in the adipose-recruited pDCs by transporting extracellular DNA via receptor for advanced glycation endproducts (RAGE) and induces production of type I interferons. Type I interferons in turn help in proinflammatory polarization of adipose-resident macrophages. Interferon signature gene expression in VAT correlates with both adipose tissue and systemic insulin resistance in obese individuals, represented by ADIPO-IR and HOMA2-IR respectively, and defines two subgroups with different susceptibility to insulin resistance. Thus our study reveals a hitherto unknown pathway that drives adipose tissue inflammation and consequent insulin resistance in obesity.

Word count: 163

Obesity and associated metabolic disorders are major health problems worldwide. Studies done over the past decade or so have established that the visceral adipose tissue (VAT) in the obese individuals harbors chronic low-grade inflammation, termed metaflammation, involving myriad innate and adaptive immune cell subsets(1,2,3). Interest in mechanisms of metaflammation grew after discovery of resident macrophages in visceral adipose tissue of obese individuals (4). The chemokine-receptor axis CCL2-CCR2 has been implicated in the recruitment of monocyte-derived macrophages into the adipose tissue (5,6). In obese VAT, as opposed to lean VAT, the resident macrophages show a classically activated proinflammatory M1 phenotype rather than so-called alternatively activated anti-inflammatory M2 phenotype (2). Although CCR2⁺ macrophages has been shown to get recruited in response to CCL2 expressed in obese VAT, there is no evidence for selective recruitment of M1 macrophages in response to CCL2. A recent study shows that CCL2 rather promotes a M2 phenotype (7). Thus switch in macrophage phenotype in response to hyperadiposity cannot be explained by the CCL2-CCR2 axis. Therefore the potential mediators for the M2 to M1 switch are probably induced in obese VAT *in situ*. One of the proposed candidates is circulating free fatty acid (FFA), which has the potential of inducing proinflammatory cytokine production from adipocytes via toll-like receptor 4 (TLR4) (8). These adipose-derived cytokines in turn can affect the macrophage phenotypic switch *in situ* as well as systemic insulin resistance (9). Fetuin-A, a fatty acid binding glycoprotein secreted from liver, has been implicated in mediating TLR4 activation by FFAs (10). Nevertheless, mechanistic link between the metabolic deregulation associated with increased adiposity and innate immune initiation of metaflammation remains largely unclear. One of the major adipose-intrinsic deregulation in obesity is change in adipokine expression levels. An imbalance between two such adipokines, leptin and adiponectin, has been found to be instrumental for the metabolic

derangements associated with obesity (11). Chemerin (expressed by tazarotene-induced gene 2 or TIG2) is another such adipokine that regulates adipocyte development, differentiation and metabolic function (12). Chemerin expression in adipocytes is increased with abundance of FFAs (13), accordingly its systemic level has been found to be elevated in obese patients with metabolic syndrome (14,15). Moreover genetic deficiency of chemokine-like receptor 1 (CMKLR1), the cognate receptor for chemerin, in mice protects them from high-fat diet (HFD)-induced insulin resistance (14). Of note, chemerin also acts as a chemokine for immune cells acting through CMKLR1, specifically for plasmacytoid dendritic cells (pDCs) (16), the major type I interferon (IFN)-producing cells in the body. In autoimmune contexts like psoriasis chemerin has been shown to recruit pDCs in tissues and initiate the cascade of autoreactive inflammation through type I IFNs (17,18,19). We wondered if adipose tissue-derived chemerin is in some way involved in linking hyperadiposity to initiation of metaflammation, by playing a similar chemotactic function in obesity as well. To investigate this, we collected visceral adipose samples from obese individuals, and by means of whole tissue gene expression, adipose explant culture and cell culture studies unraveled a hitherto unknown role of chemerin-recruited pDCs and type I interferons in the initiation of metaflammation.

RESEARCH DESIGN AND METHODS

Patients and tissue samples

We recruited 83 obese individuals and 28 lean individuals for the study, who were undergoing bariatric surgery (obese) or other abdominal surgeries (lean) at the ILS Hospitals, Kolkata, India. Relevant characteristics of the recruited patients are provided in Table 1. Greater omental

adipose tissue samples from all obese individuals and 11 lean individuals and peripheral blood samples were collected after taking written informed consent from the patients, as per recommendations of the institutional review boards of all participating institutes.

RNA isolation and quantitative Real time PCR

Total RNA was isolated from both *in vitro* cultured and *ex vivo* sorted macrophages and VAT using TRizol reagent (Life Technologies, USA), cDNA synthesized using Superscript III (Thermo Scientific, USA) and assayed for the expression of indicated genes by real time PCR (on Applied Biosystems 7500 Fast instrument) using SYBR Green master mix (Roche, Switzerland). The primers are listed in online supplemental table 1.

Isolation of stromal vascular fraction from VAT

After collection, major macroscopic blood vessels were removed by dissection from the VAT samples, followed by wash in PBS (three changes) and digestion in PBS supplemented with 0.075% Collagenase I, 1% BSA and 1% HEPES at 37°C. Stromal vascular fraction (SVF) was obtained by centrifugation of the digested VAT at 300g for 10minutes, followed by passage through 100µm cell strainer (SPL Life Sciences, South Korea).

Flow cytometric analysis and sorting

CD123⁺ CLEC4c⁺ pDCs in the stromal vascular fractions (SVF) from the VAT samples were enumerated by using fluorophore-tagged antibodies: CD45 PE (BD Bioscience, San Diego, CA), CD3 FITC, CD8 PerCP, CLEC4c APC, CD123 eFlour450 (eBioscience, Santa Clara, CA). To assess surface phenotype of *in vitro* generated macrophages, we used anti-human CD14 PerCP,

CD11b BV421, CD206 FITC and CD86 APC (BD Bioscience). Macrophage subsets in the SVF from the VAT samples (N=11) were enumerated using CD3 PerCP, CD163 APC (eBioscience), CD45-PE, CD11b-FITC, CD11c-PE Cy7 (BD Bioscience) to identify M1 (CD11b⁺ CD11c⁺) and M2 (CD11b⁺ CD163⁺) polarized macrophages by flow cytometry. In some cases (N=7) the M1 and M2 subsets were sorted on a BD FACS Aria cell sorter for subsequent gene expression studies.

Adipose Tissue sectioning and staining

Adipose tissue samples were cryo-sectioned (15µM thick) in a Leica CM1950 cryotome using Shandon cryomatrix and stained with PE conjugated BDCA4 antibody (Miltenyi Biotec, Germany). DAPI-counterstained sections were mounted with Vectashield (Vector Labs, Burlingame, CA) and 200X images were acquired on an Evos FL fluorescence microscope (Life technologies, USA).

PDC isolation and culture

PDCs were isolated from the Peripheral blood mononuclear cells (PBMCs) by magnetic immunoselection using anti-BDCA4 microbeads (Miltenyi Biotec). Isolated pDCs were cultured in complete RPMI medium (or as indicated), in 96 well U-bottom plates.

Adipose explant culture

VAT samples were collected in PBS supplemented with 1% antibiotic-antimycotic solution (Anti-Anti, Thermo Gibco, NY). Minced pieces of tissue were weighed and cultured in complete

RPMI medium (Thermo Gibco). Supernatant (Adipose Explant Culture Supernatant or AEC-sup) was collected from the culture at 1, 7, 14, 24 and 36 hours, and then cryostored.

PDC migration assay

Purified pDCs were cultured for 1 hour in RPMI medium with 2% FBS (migration medium) followed by incubation for 15 minutes in presence of control antibody (rat IgG2a, 1µg/ml, eBioscience, Santa Clara, CA) or anti-CMCLR1 antibody (1µg/ml, eBioscience), or just the migration medium. Then 50×10^3 pDCs in 100µl was added to top transwell inserts and either 600µl of AEC-sup or control medium was added to bottom chambers. After 5 hours, plate was kept on ice for 15 minutes and number of migrating cells was counted. In some experiments purified recombinant human chemerin (10 ng/ml, R&D Systems, Minneapolis, USA) were used to drive pDC migration, in presence of the anti-CMCLR1 antibody or control antibody, as described.

Reporter assays

HEK cells (70,000 cells/200µl), expressing human TLR9 along with a NF-κB promoter-driven secreted embryonic alkaline phosphatase (SEAP) reporter (Invivogen, San Diego, CA), were used for assessing TLR9 activation by the AEC-sup. 25% of total volume of adipose explant culture sup or control medium was used for the assays and the SEAP activity was assessed using Quanti-Blue Detection media (Invivogen, USA).

PDC stimulation with adipose explant culture supernatants

AEC-sups were added to pDC cultures to check for type I IFN induction. To deplete adipose explants supernatants of DNA molecules the AEC-sups were treated with 200U/ml DNase (Thermo scientific, MA, USA) for 1 hour at 37°C before addition to pDC cultures. In some experiments RAGE receptors were blocked on pDCs, using 1µg/ml anti-human RAGE goat polyclonal antibody (R&D Systems, Minneapolis, USA), before adding the AEC-sups. To deplete the HMGB1-bound TLR9 ligands, AEC-sups were added with either 5µg/ml anti-HMGB1 monoclonal antibody (R&D Systems) or control antibody or none (mock depletion), and then added to the tubes containing magnetic Protein G bead (Merck Millipore, MA, USA). Following incubation for 12 hours, the antibody-bound beads, were removed using a Magna rack. Following this, the mock and antibody-depleted supernatants were added onto freshly isolated pDCs.

Enzyme linked immunosorbent assay

ELISA was done for the detection and measurement of IFN α (Mabtech, Sweden) in the supernatants obtained from pDC cultures, TNF α in the supernatant of macrophage culture (Mabtech), chemerin (Merck-Milipore, MA, USA) in the supernatants from adipose explants culture and insulin (Merck-Milipore) in plasma samples. ELISAs were performed as per the respective manufacturer's protocol. Free fatty acid estimation was done on the plasma samples, using a flurometric assay kit (Cayman Chemical, Michigan, USA).

RNA Interference

Knock down of TLR9 expression in freshly isolated pDCs were done with siRNA using nucleofection following the manufacturer's protocol (Amaxa Lonza 4D nucleofector kit, Koln,

Germany). 5×10^5 PDCs were resuspended in 100 μ L of supplemented P3 nucleofection buffer. Control (esiRNA targeting EGFP, Sigma-Aldrich, MA, USA) or human TLR9 (sequence: GACCUCUAUCUGCACUUCUdTdT) specific siRNA (Eurogentec, Liège, Belgium) was delivered using the program FF168. After 18 hours of culture in complete RPMI medium, cells were harvested and plated in 96 well U-bottom plate and treated as indicated.

Macrophage culture

Peripheral blood CD14⁺ monocytes were isolated by magnetic immunoselection from healthy PBMCs and were differentiated to macrophages by culturing in presence of recombinant human MCSF (500U/ml, R&D system, Minneapolis, USA) in 24 well plates. 48 hours later, recombinant human IL4 (20 ng/ml, Tonbo Bioscience, San Diego, CA) was added to the macrophages to allow polarization to the M2 phenotype and incubated for an additional 48 hours (except control wells). Following this, recombinant human IFN α (PBL Interferon Source, NJ, USA) was added in indicated concentrations (10, 100, and 1000 U/ml). Cultured macrophages and their supernatants were then harvested and processed after 48 hours for further studies. In some experiments *in vitro* generated M2 macrophages (10×10^5) were co-cultured with freshly isolated autologous pDCs (10×10^4) in the presence of AEC-sups.

Statistics

Statistical analyses of all data were done on Graphpad Prism 5.0 software. Data were compared between groups using paired or unpaired Student's T test and Spearman's rank correlation as specified in respective figure legends.

RESULTS

VAT-derived chemerin recruits pDCs in obesity

We recruited adult obese individuals undergoing bariatric surgery and collected samples of their visceral adipose tissue (VAT). To explore the potential role of VAT-derived chemerin in recruitment of pDCs into VAT, we did explant cultures with human VAT samples. We found accumulation of chemerin in the adipose explant culture supernatant (hereafter mentioned as AEC-sup) with time (Figure 1A). We then checked the chemotactic function of these AEC-sup in transwell migration experiments with purified pDCs from healthy donors. Neutralizing the receptor CMKLR1 leads to total abolition of recombinant chemerin-induced pDC migration in transwell experiments (Online Supplemental Figure 1A). We found efficient pDC migration along the AEC-sup gradient and that also could be inhibited by neutralizing CMKLR1 receptor on pDCs using a monoclonal antibody (mAb), as opposed to an isotype control antibody (Figure 1B). Gene expression studies on these VAT samples revealed that VAT expression of TIG2 was not upregulated in obese as compared to lean individuals (Figure 1C). But plasma level of chemerin was significantly higher in obesity (Figure 1D). Thus it seems that the increased volume of body visceral fat, rather than intrinsic biology of the adipose tissue, is responsible for this increased plasma level of chemerin in obesity. Obese VAT also showed significantly higher enrichment of CLEC4C expression (Figure 1E), the signature transcript for pDCs (20). We found a strong positive correlation between expression of chemerin (TIG2) and CLEC4C expression (Figure 1F). . Recruitment of other immune cell subsets in response to chemerin is implausible, as expression of *CMKLR1*, the chemerin receptor, is restricted to pDCs among different immune cells (Online Supplemental Figure 1B). We isolated stromal vascular fraction from the collected

VAT samples and detected significant enrichment of CD45⁺CD3⁻CD8⁻CD123⁺BDCA2⁺ pDCs by flow cytometry, as compared to peripheral blood (Figure 1G,H). BDCA4⁺ pDCs were also detected *in situ* in cryosections of VAT (Figure 1I). These studies reveal that in obese individuals adipose-derived chemerin can recruit pDCs from circulation into the visceral adipose tissue through CMKLR1 receptor and thus link hyperadiposity-driven functional phenotype of adipocytes to recruitment of a major innate immune cell.

Type I interferon induction by VAT-recruited pDCs

pDCs are the most efficient type I IFN producing cells in the immune system (21). Induction of type I IFN production by pDCs, in response to recognition of self or nonself nucleic acid molecules by endosomal TLRs (TLR9 and TLR7), is the mainstay of pDC function in protective immunity against pathogens (mostly viruses) as well as in their key role in several autoimmune diseases (18,19,21,22,23). Finding chemerin-driven recruitment of pDCs into VAT of obese individuals naturally led to the possibility of pDC activation *in situ* and involvement of type I IFNs in metaflammation. We checked for expression of four genes (IRF7, ISG15, MX1 and TRIP14), representative of the group of signature genes expressed in responder cells in response to type I IFN signaling (Interferon Signature Genes or ISGs) that have previously been shown to be surrogate markers for type I IFN induction in several autoimmune contexts (24,25). We formulated an ISG index (ISGi) as an average of relative expressions of the four selected ISGs (Online Supplemental Figure 2A-F) and found CLEC4C expression in VAT correlates positively with ISGi (Figure 2A). As expected, ISGi was significantly higher in obese VAT as compared to lean VAT (Figure 2B).

Previous studies have established that visceral fat depots are critical sites for obesity associated metaflammation compared to subcutaneous adipose tissue (26). To confirm the importance of visceral adipose tissue in this phenomenon, we compared paired samples of subcutaneous adipose tissue (SAT) with VAT samples (N=6). As expected VAT samples showed significantly higher expression of TIG2, enrichment of CLEC4C transcript as well as ISGi (Online Supplemental Figures 3A-C).

To look for endogenous molecules that may induce type I IFN induction in VAT recruited pDCs, we added the AEC-sups, generated from explant cultures of adipose tissue collected from obese individuals, to purified pDCs from healthy donors in culture. We found that AEC-sups could induce type I IFN production by pDCs (Figure 2C). When AEC-sups were treated with DNase before addition to the culture, this pDC activation was abrogated, indicating that extracellular DNA molecules released in the AEC-sup play a role in this pDC activation (Figure 2D). Relative abundance of extracellular nucleic acids in visceral adipose tissue can be extrapolated from the higher propensity of adipocyte death and tissue remodeling previously reported in obesity (27,28). AEC-sups were also able to trigger TLR9 activation in HEK293 cells that express TLR9 and report downstream NF κ B activation through an enzymatic reporter (Figure 2E). When TLR9 gene was knocked down in pDCs using siRNAs (Online Supplemental Figure 4A), AEC-sup-induced type I IFN production by pDCs was abolished (Figure 2F), confirming critical role of TLR9 activation in this event.

HMGB1 aids activation of VAT-recruited pDCs

Under physiological conditions extracellular nucleic acids of self-origin cannot access the TLRs in pDCs due to their endosomal localization (21). But in autoimmune contexts endogenous

molecules (e.g LL37, HMGB1 etc.) take part in transport of self nucleic acids into pDC endosomes and initiate sterile autoreactive inflammation (21,19). Among such molecules the high mobility group B1 (HMGB1) protein has been shown to bind extracellular self-DNA molecules and facilitate their recognition by pDC endosomal TLR9, through participation of the receptor for advanced glycation end-products (RAGE), which is expressed in pDCs (29). Interestingly, in a recent study it was shown that in obese individuals there is elevated level of HMGB1 in plasma as well as an increased expression in VAT, which correlated with the adipose inflammatory markers (30). So we speculated that HMGB1 may help in TLR activation in VAT-recruited pDCs. Antibody-mediated neutralization of the HMGB1 receptor RAGE on pDCs could inhibit AEC-sup-induced type I IFN induction (Figure 3A). Moreover, antibody-mediated depletion of HMGB1 from the AEC-sup, before they were added to pDC cultures, abolished the type I IFN induction capability of the AEC-sup (Figure 3B). Similar mechanism of pDC activation seems to operate *in vivo* in obese patients as well. We found a significantly positive correlation between expression of *HMGB1* and ISGi in VAT samples (Figure 3C). Thus we find that adipose tissue derived HMGB1 and extracellular self-DNA molecules trigger TLR9 activation in pDCs aided by RAGE receptors on pDCs, leading to induction of type I IFN production *in situ*.

Type I interferons polarize macrophages to a proinflammatory phenotype

A mechanistic link between accumulation and proinflammatory polarization of macrophages in the visceral adipose tissue is established in obesity associated metaflammation (3,4,31). Macrophages in lean adipose tissue show an ‘alternatively activated’ anti-inflammatory ‘M2’ phenotype, while in obese adipose tissue they show ‘classically activated’ proinflammatory ‘M1’

phenotype (3,31). Whether this results from selective recruitment of M1-like macrophages into VAT or due to *in situ* polarization of M2 to the M1 phenotype remains an open question. We wanted to explore whether type I IFN induction in VAT can drive *in situ* polarization of M2 macrophages to the proinflammatory M1 phenotype. First to check if this can happen *in vitro*, we generated M2 macrophages from CD14⁺ monocytes isolated from peripheral blood of healthy individuals in presence of MCSF and IL-4. We found these *in vitro* generated M2 macrophages could be polarized to a proinflammatory M1-like phenotype in presence of recombinant IFN α in terms of reduction in expression of M2-specific genes like F13A1, CCL22 (Figures 4A,B) and surface expression of the mannose receptor, CD206, an established marker for M2 macrophages generated *in vitro* in response to IL4 (32) (Figure 4E,F). Expression of IRF5 (interferon regulatory factor 5), a transcription factor with established role in proinflammatory polarization of macrophages (33,34), and NOS2, the gene for inducible nitric oxide synthase that is characteristically expressed in M1 macrophages, were increased in presence of IFN α (Figure 4C,D). Surface expression of the costimulatory molecule CD86, characteristic of M1-like proinflammatory macrophages (35), was also enhanced in presence of IFN α (Figure 4E,F). There was also enhancement of constitutive TNF α production in the macrophage cultures in presence of IFN α (Figure 4G). Thus we found that IFN α , the major member of type I IFN family, can drive polarization of alternatively activated macrophages to a proinflammatory phenotype *in vitro*.

Role of type I interferons in macrophage polarization *in situ*

To confirm the role of pDCs in polarization of M2 to M1 macrophages in response to VAT-derived TLR9 ligands, we performed co-culture experiments of *in vitro* generated M2

macrophages and freshly isolated pDCs in presence of AEC-sup (Figure 5A). We found that the proinflammatory polarization of the M2 macrophages in response to AEC-sup was significantly reduced in the absence of co-cultured pDCs, in terms of surface expression of M2-specific marker CD206 (Figure 5B) and M1 specific marker CD86 (Figure 5C). This was associated with significant reduction in accumulation of IFN α in the supernatant (Figure 5D).

To further validate the putative role of type I IFN response in *in situ* M1 polarization of the VAT-resident macrophages, we isolated M1-type and M2-type resident macrophages from the stromal vascular fractions of VAT from obese individuals by flow cytometric sorting. Expression of surface markers CD206 and CD86, used for assessing *in vitro* generation of M1 and M2 phenotypes, did not distinguish these phenotypic subsets in SVF, which is not surprising as characteristic markers of macrophage subsets vary between contexts (36). Adipose tissue resident M2 macrophages can be identified by expression of CD163, while M1 macrophages present in obese VATs express CD11c (35,37,38). Accordingly, we could define distinct subsets of M1 and M2 macrophages in SVF isolated from VAT samples as CD45⁺ CD11b⁺ CD11c⁺ and CD45⁺ CD11b⁺ CD163⁺ cells respectively (Figure 5E). Apart from the surface markers, the subsets could also be validated based on expression IRF5 (Figure 5F) and NOS2 (Figure 5G). We found that expression of the ISG genes were significantly enriched in the CD11c⁺ M1 subset (Figure 5H), indicating that a type I IFN response in the adipose resident macrophages favors M1 polarization. The expression of IRF5 and NOS2 in the CD11c⁺ M1 macrophages strongly correlated with ISGi values as well (Figures 5I,J).

In few recent studies, done in murine models of high fat diet (HFD)-induced metabolic syndrome, TLR9 activation in macrophages in response to circulating DNA has been implicated in proinflammatory polarization of macrophages (39,40). But in humans TLR9 expression is

restricted to pDCs and B cells, with no considerable expression in the myeloid compartments, as opposed to mice (41). To confirm this we also compared expression of TLR9 in circulating pDCs, B cells, T cells, conventional dendritic cells, monocytes as well as *in vitro* generated and *ex vivo* isolated M1 and M2 macrophages. We found pDCs as the major TLR9 expressing cells with no significant expression in any of the myeloid cell subset, as previously described (Online Supplemental Figure 4B). In whole tissue transcripts from VAT too, expression of genes characteristic of M1 macrophages, viz. IRF5 was found to be significantly correlated with the level of type I IFN induction (in terms of ISGi values) in VAT (Figure 6A) as well as expression of the pDC signature gene CLEC4C (Figure 6B). Although a significantly coherent expression of IRF5 and NOS2 *in VAT* validated their selection as M1 signature genes (Online Supplemental Figure 5A), in total VAT transcript analysis NOS2 expression was not correlated with ISGi, perhaps due to a type I IFN-independent regulation of its expression in cells other than macrophages *in vivo* (Online Supplemental Figure 5B). The ratio of frequency of M1 and M2 macrophages in the stromal vascular fraction from VATs (N=11) was also found to be correlated with VAT ISGi (Figure 6C). Thus we find that induction of type I IFNs in VAT of obese individuals drive *in situ* proinflammatory polarization of macrophages as characterized by key signature genes and surface markers, thereby fueling metaflammation.

Type I IFN induction in VAT is associated with insulin resistance

As proinflammatory polarization of VAT-recruited macrophages have been linked to systemic insulin resistance in numerous previous studies (3,31), we expected a link between level of type I IFN induction in obese VAT with adipose tissue and systemic insulin resistance. We assessed adipose tissue insulin resistance in the recruited obese individuals by measuring ADIPO-IR

index (ADIPO-IR = plasma free fatty acids x insulin concentration) which has been validated previously for this purpose (42). Interestingly, we identified two distinct groups of individuals when VAT ISGi was correlated with ADIPO-IR values in the respective individuals, in both of which ADIPO-IR values had significant positive correlation with VAT ISGi (Figure 7A-C). But one group (designated group L) had higher values ADIPO-IR corresponding to their ISGi values than the other group (group R). We also found significant positive correlation of HOMA2-IR values (indicative of systemic insulin resistance) with VAT ISGi in both groups L and R (Figure 7D,E). These groups were not significantly different with respect to body mass index (Online Supplemental Figures 6A), but group R showed significantly higher enrichment of the pDC-specific transcript CLEC4C, higher ISGi as well as higher expression of the M1 macrophage signature IRF5 (Online Supplemental Figures 6B-D). These two distinct groups perhaps point to different susceptibility of obese individuals to development of insulin resistance following the innate initiation of metaflammation through type I IFNs. Of note, level of glycated hemoglobin (HbA1c) was significantly correlated with only group R (Figure 7F), indicating higher levels of ISGi have greater influence on long term glycemic control.

Thus we unraveled a hitherto unknown pathway for initiation of metaflammation that links obesity-induced functional changes in the visceral adipose tissue with recruitment and activation of a major innate immune mechanism, which can both initiate and fuel metaflammation, as shown in the pathogenetic model (Figure 7G).

DISCUSSION

Despite recent advances in the understanding of the adipose tissue inflammation and its role in insulin resistance, all the key contributions from the immune cell subsets are yet to be understood fully. Although Fetuin-A-TLR4 axis in adipocytes and resulting macrophage chemoattractant protein 1 (MCP1) expression in visceral fat depots has been implicated in recruitment of circulating CCR2⁺ monocytes into VAT, mechanism of their polarization into proinflammatory macrophages is not clear, as discussed earlier. In our study we found that chemerin, an adipokine shown to be produced by adipocytes in response to free fatty acids with reported abundance in plasma in obese individuals, has a role in the innate initiation of the VAT inflammation. Chemerin is known to have chemoattractant property to cells expressing its cognate receptor CMKLR1, which is preferentially expressed on the plasmacytoid dendritic cells among immune cells. We think as the VAT depots become a source of chemerin in obesity, circulating pDCs infiltrate VAT in response to CMKLR1 triggering, thus linking hyperadiposity to VAT-recruitment of an innate immune cell. Although obese individuals had significantly higher level of chemerin in plasma as compared to lean individuals, VAT expression of chemerin (TIG2) showed no difference between these two groups. This indicates a dependence of systemic abundance of chemerin on total volume of VAT rather than change in adipose biology in obesity. Total VAT volume has also been shown previously to be linked with extent of inflammation (26). As expected both enrichment of the pDC transcript CLEC4C expression in VAT and ISGi was significantly higher in obese compared to lean individuals. Of note, we did not find any correlation between body mass index with plasma chemerin levels in obese individuals. This may have resulted from ongoing therapy with anti-diabetic drugs, especially metformin, in a large number of these individuals, because reduction in level of chemerin in response to drug therapy is known (43).

CD11c⁺ dendritic cell (DC) recruitment into VAT has been previously reported, but these studies focused mainly on conventional DCs (cDCs) and their role in T cell polarization. DC infiltration into the VAT and liver has also been correlated with macrophage infiltration in HFD-fed (HFDF) mouse, which reduced in animals genetically deficient in CD11c⁺ DCs (44). Although in this study VAT-infiltrating DCs comprised of both cDCs and pDCs, the phenotype was linked to the role of cDCs (44). Another study provided evidence for CD11c⁺ cell recruitment in VAT of obese individuals and also showed that ablation of CD11c⁺ DCs in HFDF obese mice reduced VAT inflammation as well as insulin resistance (45). But the reason behind this recruitment of DCs and initiation of the metaflammation process was not clear in any of the studies.

PDCs are the major producers of type I IFNs in the body (21) and role of pDC-derived type I IFNs in initiating autoreactive inflammation in several autoimmune disease is well established (22,18,19,23). In our study we show the possible mechanism of activation of VAT-recruited pDCs by free self-DNA molecules released from the adipose tissue. PDC activation and consequent type I IFN induction was dependent on HMGB1 bound to the DNA molecules and RAGE receptor on pDCs. Recent findings of amelioration of disease in HFDF mice with genetic deficiency of RAGE (46), as well as increased concentration of circulating HMGB1 in obese individuals with metabolic syndrome (30), support this possibility. An increased adipose tissue turnover and adipocyte death in obese individuals can be responsible for abundance of both HMGB1 and the free nucleic acid molecules.

TLR9 recognises unmethylated CpG motifs on DNA molecules (21). Both genomic and mitochondrial DNA do contain such motifs, and their release in response to adipocyte death can trigger TLR9 activation in pDCs, when aided by molecules like HMGB1. Recently plasma from both HFDF mice as well as patients with nonalcoholic steatohepatitis was shown to have circulating mitochondrial DNA, which contributes to hepatic inflammation and disease through TLR9 triggering (39). A more recent study showed TLR9 activation in VAT-recruited macrophages in response to cell free DNA from dying adipocytes induced CCL2 expression *in situ* (40). Accordingly in TLR9^{-/-} HFDF mice accumulation of macrophages in VAT, VAT-resident inflammation as well as insulin resistance was attenuated. Interestingly, in both these murine studies the whole phenotype was shown to be dependent on TLR9 expression in lysozyme expressing macrophages, while in humans TLR9 expression is largely restricted in pDCs and B cells (41). The second study also found that level of circulating DNA molecules, the TLR9 ligands, was increased in obese individuals and correlated with their systemic insulin resistance (40).

In clinical contexts of autoimmune disorders, pDC-derived type I IFNs drive inflammation by influencing cDC maturation as well as potentiation of autoreactive B cell activation and expansion (47,48). We now unravel a direct action of type I IFNs on the VAT recruited macrophages. We provide evidence of polarization of M2 macrophages to proinflammatory M1 phenotype in response to type I IFNs both *in vitro* and *in situ*. The phenotypic details of *in vitro* generated and *ex vivo* isolated macrophages were somewhat different in terms of gene expression and surface markers, probably due to additional microenvironmental factors *in vivo*. Among the *ex vivo* isolated macrophages we could identify and isolate CD163⁺ M2 and CD11c⁺ M1 subsets as described (2). The *ex vivo* isolated M1 macrophages had a clear enrichment of interferon

signature gene expression. In a previous study, again in HFDF mouse model, CD11c⁺ macrophages were shown to be instrumental for the adipose inflammation and insulin resistance (49), as shown by disease amelioration on genetic deficiency of CD11c⁺ cells. But in that study the phenotype might have contributions from both infiltrating DCs (pDCs and cDCs) as well as M1 macrophages, as all of them express CD11c.

VAT-infiltration of a number of other immune cells has been implicated in metaflammation, other than macrophages and dendritic cells (3,50). The cellular components of the adaptive immune system, viz. Th1-polarized CD4 cells (51) and cytotoxic CD8 T cells (52), perhaps get involved downstream of innate initiation of metaflammation. But recently *in situ* activation of VAT-resident NK cells, an innate immune cell subset, was found to be critical driver of metaflammation in independent studies using two different genetic models of NK cell deficiency, as well as in human obese individuals (53,54). Of note here, a critical role of type I IFNs is established in regulation of NK cell function in contexts like viral infection and solid tumors (55,56,57). A recent study also established that NK cell activation and survival is severely impaired in the absence of type I IFNs (58). Thus plausibly *in situ* induction of type I IFNs in VAT, as reported by us, mechanistically precedes activation of NK cells during metaflammation.

We found that induction of type I IFN in VAT was linked to both adipose tissue (represented by ADIPO-IR) and systemic insulin resistance (represented by HOMA2-IR), although it was not correlated individually with fasting blood glucose, free fatty acid or insulin levels in plasma (data not shown). Interestingly, we could identify two subgroups among obese individuals with different susceptibility of insulin unresponsiveness in the adipose tissue to the level of type I IFN

induction *in situ*. The left shifted group (group L) had higher ADIPO-IR levels at lower VAT ISGi compared to the right shifted group R. HOMA2-IR was similarly regulated in response to VAT ISGi. Of note, level of HbA1c was correlated with VAT ISGi only in group R perhaps pointing to higher ISGi levels affecting long term glycemic control to a greater extent.

A putative role of type I IFNs in systemic insulin resistance had been suggested long back in a study where human subjects injected with IFN α developed insulin resistance (59). Pegylated IFN α therapy in patients with HCV infection was also found to be associated with insulin resistance (60,61). In a recent study genetic deficiency of IRF7 (interferon regulatory factor 7), the critical transcription factor for induction of type I IFNs in pDCs (62), was found to protect mice from HFD-induced metabolic syndrome (63). In clinical contexts, an associated risk of developing metabolic disorders has already been established in systemic lupus erythamatosus (64) and psoriasis (65), where pDC-derived type I IFNs play a central role in pathogenesis (19). Interestingly, administration of hydroxychloroquine (HCQ), the anti-malarial drug with anti-rheumatic effects, was found to improve insulin sensitivity in obese individuals (66,67). Role of HCQ in inhibition of endosomal TLRs, either by regulation of endosomal acidification or direct interaction with the nucleic acid ligands, is established (68,69). We speculate that the anti-diabetic effect of HCQ is also through inhibition of TLR-mediated type I IFN induction. Of note here, level of systemic insulin resistance represents both the influence of metaflammation and intrinsic insulin unresponsiveness in metabolically active tissues. Thus, beyond its contribution to metaflammation, the role of type I IFNs in driving systemic insulin resistance by direct action on metabolically active tissues needs to be explored. Actually, suggestion of hepatic insulin resistance in response to IFN α has already been made in a previous study (70).

Altogether, we propose a novel model (Figure 7G) for initiation of metaflammation in obese individuals, wherein adipose recruitment of pDCs in response to high expression of chemerin, and *in situ* TLR activation in the adipose-recruited pDCs in response to HMGB1-nucleic acid complexes, lead to induction of type I IFNs. Type I IFNs in turn fuel metaflammation by driving proinflammatory polarization of macrophages in visceral adipose tissue and contribute to systemic insulin resistance. Type I IFNs are already being explored as therapeutic targets in different systemic autoimmune contexts (71,72). Our study opens up the possibility of similar therapeutic approaches in obesity associated metabolic syndrome as well.

AUTHOR CONTRIBUTIONS

D.G. conceptualized the project, designed the experiments; A.R.G. performed most of the experiments; T.C., S.K. and O.T. recruited and performed bariatric surgical procedures on obese patients; R.B. and S.R. performed pDC activation studies; R.B., S.B., O.R., D.R.C., C.S.C.L. participated in gene expression studies; TN participated in SVF studies; S.B. participated in the flow cytometry; R.B., T.N., P.D., P.G., C.S.C.L. participated in patient sample and data collection; P.G., S.H., S.M., P.C. participated in clinical evaluation and stratification of recruited patients; D.G., A.R.G., P.C. and S.H. analyzed the data; D.G. and A.R.G. wrote the manuscript.

ACKNOWLEDGEMENTS

The study was supported by Ramanujan Fellowship grant from Department of Science & Technology (Govt. of India) and network project grant BSC0114 from Council of Scientific &

Industrial Research (CSIR) awarded to DG and network project grant BSC0206 from CSIR awarded to PC; ARG and OR are supported by Senior Research Fellowships from University Grants Commission, India; RB and TN receive CSIR Senior Research Fellowships; DRC and CSCL are supported by CSIR-Junior Research Fellowships; SB is supported by Research Associateship from Department of Biotechnology (Govt. of India). We thank Utpalendu Ghosh and Suvendra Nath Bhattacharyya (CSIR-Indian Institute of Chemical Biology) for help with cryosections and nucleofection experiments respectively. The corresponding author takes full responsibility for the work as a whole, including the study design, access to data, and the decision to submit and publish the manuscript.

SUPPLEMENTAL INFORMATION

Supplemental information includes six online supplemental figures and one table .

CONFLICT OF INTEREST

Authors declare no conflict of interest.

REFERENCES

1. Gregor MF, Hotamisligil GS. Inflammatory mechanisms in obesity. *Annual Reviews in Immunology* 2011; 29: 415-445.
2. Chawla A, Nguyen KD, Goh YP. Macrophage-mediated inflammation in metabolic disease. *Nature Reviews Immunology* 2011; 11(11):738-49.
3. Mathis D. Immunological goings-on in visceral adipose tissue. *Cell Metabolism* 2013; 17: 851-859.
4. Weisberg SP, McCann D, Desai M, Rosenbaum M, Leibel RL, Ferrante AW Jr. Obesity is associated with macrophage accumulation in adipose tissue. *Journal of Clinical Investigation* 2003; 112: 1796-1808.
5. Weisberg SP, Hunter D, Huber R, Lemieux J, Slaymaker S, Vaddi K, Charo I, Leibel RL, Ferrante AW Jr. 2006. CCR2 modulates inflammatory and metabolic effects of high-fat feeding. *Journal of Clinical Investigation* 2006; 116: 115-124.
6. Oh DY, Morinaga H, Talukdar S, Bae EJ, Olefsky JM. Increased macrophage migration into adipose tissue in obese mice. *Diabetes* 10.2337/db11-0860.
7. Sierra-Filardi E, Nieto C, Domínguez-Soto A, Barroso R, Sánchez-Mateos P, Puig-Kroger A, López-Bravo M, Joven J, Ardavín C, Rodríguez-Fernández JL, Sánchez-Torres C, Mellado M, Corbí AL. CCL2 shapes macrophage polarization by GM-CSF and M-CSF: identification of CCL2/CCR2-dependent gene expression profile. *Journal of Immunology* 2014; 192: 3858-3867.
8. Shi H, Kokoeva MV, Inouye K, Tzameli I, Yin H, Flier J.S. 2006. TLR4 links innate immunity and fatty acid-induced insulin resistance. *Journal of Clinical Investigation* 2006; 116: 3015-3025.

9. Kim JK. Fat uses a TOLL-road to connect inflammation and diabetes. *Cell Metabolism* 2006 4: 417-419.
10. Pal D, Dasgupta S, Kundu R, Maitra S, Das G, Mukhopadhyay S, Ray S, Majumdar SS, Bhattacharya S. 2012. Fetuin-A acts as an endogenous ligand of TLR4 to promote lipid-induced insulin resistance. *Nature Medicine*. 18: 1279-1285.
11. Ouchi N, Parker JL, Lugus JJ, Walsh K. Adipokines in inflammation and metabolic disease. *Nature Reviews Immunology* 2011; 11: 85-97.
12. Ernst MC, Sinal CJ. Chemerin: at the crossroads of inflammation and obesity. *Trends in Endocrinology & Metabolism* 2010; 21: 660-667.
13. Bauer S, Wanninger J, Schmidhofer S, Weigert J, Neumeier M, Dorn C, Hellerbrand C, Zimara N, Schäffler A, Aslanidis C, Buechler C. Sterol regulatory element-binding protein 2 (SREBP2) activation after excess triglyceride storage induces chemerin in hypertrophic adipocytes. *Endocrinology* 2011; 152: 26-35.
14. Ernst MC, Haidl ID, Zúñiga LA, Dranse HJ, Rourke JL, Zabel BA, Butcher EC, Sinal CJ. Disruption of the chemokine-like receptor-1 (CMKLR1) gene is associated with reduced adiposity and glucose intolerance. *Endocrinology* 2012; 153: 672-682.
15. Li Y, Shi B, Li S. Association between serum chemerin concentrations and clinical indices in obesity or metabolic syndrome: a meta-analysis. *PLoS One* 2014; 9: e113915.
16. Zabel BA, Silverio AM, Butcher EC. Chemokine-like receptor 1 expression and chemerin-directed chemotaxis distinguish plasmacytoid from myeloid dendritic cells in human blood. *Journal of Immunology* 2005; 174: 244-251.
17. Vermi W, Riboldi E, Wittamer V, Gentili F, Luini W, Marrelli S, Vecchi A, Franssen JD, Communi D, Massardi L, Sironi M, Mantovani A, Parmentier M, Facchetti F, Sozzani S. Role

- of ChemR23 in directing the migration of myeloid and plasmacytoid dendritic cells to lymphoid organs and inflamed skin. *Journal of Experimental Medicine* 2005; 201: 509-515.
18. Ganguly D, Chamilos G, Lande R, Gregorio J, Meller S, Facchinetti V, Homey B, Barrat FJ, Zal T, Gilliet M. Self-RNA-antimicrobial peptide complexes activate human dendritic cells through TLR7 and TLR8. *Journal of Experimental Medicine* 2009; 206: 1983-1994.
19. Ganguly D, Haak S, Sisirak V, Reizis B. The role of dendritic cells in autoimmunity. *Nature Reviews Immunology* 2013; 13: 566-577.
20. Dzionek A, Sohma Y, Nagafune J, Cella M, Colonna M, Facchetti F, Günther G, Johnston I, Lanzavecchia A, Nagasaka T, Okada T, Vermi W, Winkels G, Yamamoto T, Zysk M, Yamaguchi Y, Schmitz J. BDCA-2, a novel plasmacytoid dendritic cell-specific type II C-type lectin, mediates antigen capture and is a potent inhibitor of interferon alpha/beta induction. *Journal of Experimental Medicine* 2001; 194: 1823-1834.
21. Gilliet M, Cao W, Liu YJ. 2008. Plasmacytoid dendritic cells: sensing nucleic acids in viral infection and autoimmune diseases. *Nature Reviews Immunology* 2008; 8: 594-606.
22. Lande R, Gregorio J, Facchinetti V, Chatterjee B, Wang YH, Homey B, Cao W, Wang YH, Su B, Nestle FO, Zal T, Mellman I, Schröder JM, Liu YJ, Gilliet M. Plasmacytoid dendritic cells sense self-DNA coupled with antimicrobial peptide 2007; *Nature*. 449: 564-569.
23. Sisirak V, Ganguly D, Lewis KL, Couillault C, Tanaka L, Bolland S, D'Agati V, Elkon KB, Reizis B. Genetic evidence for the role of plasmacytoid dendritic cells in systemic lupus erythematosus. *Journal of Experimental Medicine* 2014; 211: 1969-1976.
24. Bennett L, Palucka AK, Arce E, Cantrell V, Borvak J, Banchereau J, Pascual V. Interferon and granulopoiesis signatures in systemic lupus erythematosus blood. *Journal of Experimental Medicine* 2003; 197: 711-723.

25. Rönnblom L, Eloranta ML. The interferon signature in autoimmune diseases. *Current Opinions in Rheumatology* 2103;25: 248-253.
26. Sam S, Haffner S, Davidson MH, D'Agostino RB Sr, Feinstein S, Kondos G, Perez A, Mazzone T. Relation of abdominal fat depots to systemic markers of inflammation in type 2 diabetes. *Diabetes Care* 2009; 32: 932-937.
27. Cinti S, Mitchell G, Barbatelli G, Murano I, Ceresi E, Faloia E, Wang S, Fortier M, Greenberg AS, Obin MS. Adipocyte death defines macrophage localization and function in adipose tissue of obese mice and humans. *Journal of Lipid Research* 2005; 46: 2347-2355.
28. Strissel KJ, Stancheva Z, Miyoshi H, Perfield JW 2nd, DeFuria J, Jick Z, Greenberg AS, Obin MS. 2007. Adipocyte death, adipose tissue remodeling, and obesity complications. *Diabetes* 2007; 56: 2910-2918.
29. Tian J, Avalos AM, Mao SY, Chen B, Senthil K, Wu H, Parroche P, Drabic S, Golenbock D, Sirois C, Hua J, An LL, Audoly L, La Rosa G, Bierhaus A, Naworth P, Marshak-Rothstein A, Crow MK, Fitzgerald KA, Latz E, Kiener PA, Coyle AJ. Toll-like receptor 9-dependent activation by DNA-containing immune complexes is mediated by HMGB1 and RAGE. *Nature Immunology* 2007; 8: 487-496.
30. Guzmán-Ruiz R, Ortega F, Rodríguez A, Vázquez-Martínez R, Díaz-Ruiz A, Garcia-Navarro S, Giralt M, Garcia-Rios A, Cobo-Padilla D, Tinahones FJ, López-Miranda J, Villarroya F, Frühbeck G, Fernández-Real JM, Malagón MM. 2014. Alarmin high-mobility group B1 (HMGB1) is regulated in human adipocytes in insulin resistance and influences insulin secretion in β -cells. *International Journal of Obesity* 2014; 38: 1545-1554.
31. Odegaard JI, Chawla A. 2013. Pleiotropic actions of insulin resistance and inflammation in metabolic homeostasis. *Science* 2013; 339: 172-177.

32. Stein M, Keshav S, Harris N, Gordon S. Interleukin 4 potently enhances murine macrophage mannose receptor activity: a marker of alternative immunologic macrophage activation. *Journal of Experimental Medicine* 1992; 176: 287-292.
33. Krausgruber T, Blazek K, Smallie T, Alzabin S, Lockstone H, Sahgal N, Hussell T, Feldmann M, Udalova IA. IRF5 promotes inflammatory macrophage polarization and TH1-TH17 responses. *Nature Immunology* 2011; 12: 231-238.
34. Dalmas E, Toubal A, Alzaid F, Blazek K, Eames HL, Lebozec K, Pini M, Hainault I, Montastier E, Denis RG, Ancel P, Lacombe A, Ling Y, Allatif O, Cruciani-Guglielmacci C, André S, Viguerie N, Poitou C, Stich V, Torcivia A, Foufelle F, Luquet S, Aron-Wisnewsky J, Langin D, Clément K, Udalova IA, Venteclef N. Irf5 deficiency in macrophages promotes beneficial adipose tissue expansion and insulin sensitivity during obesity. *Nature Medicine* 2015; 21: 610-618.
35. Shaul ME, Bennett G, Strissel KJ, Greenberg AS, Obin MS. Dynamic, M2-like remodeling phenotypes of CD11c⁺ adipose tissue macrophages during high-fat diet-induced obesity in mice. *Diabetes* 2010; 59 :1171-1181.
36. Murray PJ, Allen JE, Biswas SK, Fisher EA, Gilroy DW, Goerdt S, Gordon S, Hamilton JA, Ivashkiv LB, Lawrence T, Locati M, Mantovani A, Martinez FO, Mege JL, Mosser DM, Natoli G, Saeij JP, Schultze JL, Shirey KA, Sica A, Suttles J, Udalova I, van Ginderachter JA, Vogel SN, Wynn TA. Macrophage activation and polarization: nomenclature and experimental guidelines. *Immunity* 2014; 41: 14-20.
37. Ito A, Suganami T, Yamauchi A, Degawa-Yamauchi M, Tanaka M, Kouyama R, Kobayashi Y, Nitta N, Yasuda K, Hirata Y, Kuziel WA, Takeya M, Kanegasaki S, Kamei Y, Ogawa Y. Role of

- CC chemokine receptor 2 in bone marrow cells in the recruitment of macrophages into obese adipose tissue. *Journal of Biological Chemistry* 2008; 283: 35715-35723.
38. Murray PJ, Wynn TA. Protective and pathogenic functions of macrophage subsets. *Nature Review Immunology* 2011; 11: 723-737.
39. Garcia-Martinez I, Santoro N, Chen Y, Hoque R, Ouyang X, Caprio S, Shlomchik MJ, Coffman RL, Candia A, Mehal WZ. Hepatocyte mitochondrial DNA drives nonalcoholic steatohepatitis by activation of TLR9. *Journal of Clinical Investigation* 2016; 126: 859-864.
40. Nishimoto S, Fukuda D, Higashikuni Y, Tanaka K, Hirata Y, Murata C, Kim-Kaneyama JR, Sato F, Bando M, Yagi S, Soeki T, Hayashi T, Imoto I, Sakaue H, Shimabukuro M, Sata M. Obesity-induced DNA released from adipocytes stimulates chronic adipose tissue inflammation and insulin resistance. *Science Advance* 2016; 2: e1501332.
41. Hornung V, Rothenfusser S, Britsch S, Krug A, Jahrsdörfer B, Giese T, Endres S, Hartmann G. Quantitative expression of toll-like receptor 1-10 mRNA in cellular subsets of human peripheral blood mononuclear cells and sensitivity to CpG oligodeoxynucleotides. *Journal of Immunology* 2002; 168: 4531-4537.
42. Lomonaco R, Ortiz-Lopez C, Orsak B, Webb A, Hardies J, Darland C, Finch J, Gastaldelli A, Harrison S, Tio F, Cusi K. Effect of adipose tissue insulin resistance on metabolic parameters and liver histology in obese patients with nonalcoholic fatty liver disease. *Hepatology* 2012; 55: 1389-1397.
43. Tan BK, Chen J, Farhatullah S, Adya R, Kaur J, Heutling D, Lewandowski KC, O'Hare JP, Lehnert H, Randeve HS. Insulin and metformin regulate circulating and adipose tissue chemerin. *Diabetes* 2009; 58: 1971-1977.

44. Stefanovic-Racic M, Yang X, Turner MS, Mantell BS, Stolz DB, Sumpter TL, Sipula IJ, Dedousis N, Scott DK, Morel PA, Thomson AW, O'Doherty RM. Dendritic cells promote macrophage infiltration and comprise a substantial proportion of obesity-associated increases in CD11c+ cells in adipose tissue and liver. *Diabetes* 2012; 61: 2330-2339.
45. Bertola A, Ciucci T, Rousseau D, Bourlier V, Duffaut C, Bonnafous S, Blin-Wakkach C, Anty R, Iannelli A, Gugenheim J, Tran A, Bouloumié A, Gual P, Wakkach A. Identification of adipose tissue dendritic cells correlated with obesity-associated insulin-resistance and inducing Th17 responses in mice and patients. *Diabetes* 2012; 61: 2238-2247.
46. Song F, Hurtado del Pozo C, Rosario R, Zou YS, Ananthakrishnan R, Xu X, Patel PR, Benoit VM, Yan SF, Li H, Friedman RA, Kim JK, Ramasamy R, Ferrante AW Jr, Schmidt AM. RAGE regulates the metabolic and inflammatory response to high-fat feeding in mice. *Diabetes* 2014; 63: 1948-1965.
47. Blanco P, Palucka AK, Gill M, Pascual V, Banchereau J. Induction of dendritic cell differentiation by IFN-alpha in systemic lupus erythematosus. *Science* 2001; 294: 1540-1543.
48. Braun D, Caramalho I, Demengeot J. IFN-alpha/beta enhances BCR-dependent B cell responses. *International Immunology* 2002; 14: 411-419.
49. Patsouris D, Li PP, Thapar D, Chapman J, Olefsky JM, Neels JG. Ablation of CD11c-positive cells normalizes insulin sensitivity in obese insulin resistant animals. *Cell Metabolism*. 2008; 8: 301-309.
50. Lackey DE, Olefsky JM. Regulation of metabolism by the innate immune system. *Nature Review Endocrinology* 2016; 12: 15-28.

51. Zuniga LA, Shen WJ, Joyce-Shaikh B, Pyatnova EA, Richards AG, Thom C, Andrade SM, Cua DJ, Kraemer FB, Butcher EC. IL-17 regulates adipogenesis, glucose homeostasis, and obesity. *Journal of Immunology* 2010; 185: 6947–6959.
52. Nishimura S, Manabe I, Nagasaki M, Eto K, Yamashita H, Ohsugi M, Otsu M, Hara K, Ueki K, Sugiura S, et al. CD8⁺ effector T cells contribute to macrophage recruitment and adipose tissue inflammation in obesity. *Nature Medicine* 2009; 15: 914–920.
53. Wensveen FM, Jelencic V, Valentic S, Šestan M, Wensveen TT, Theurich S, Glasner A, Mendrila D, Štimac D, Wunderlich FT, Brüning JC, Mandelboim O, Polic B. NK cells link obesity-induced adipose stress to inflammation and insulin resistance. *Nature Immunology* 2015; 16: 376-385.
54. Lee BC, Kim MS, Pae M, Yamamoto Y, Eberlé D, Shimada T, Kamei N, Park HS, Sasorith S, Woo JR, You J, Mosher W, Brady HJ, Shoelson SE, Lee J. Adipose Natural Killer Cells Regulate Adipose Tissue Macrophages to Promote Insulin Resistance in Obesity. *Cell Metabolism* 2016; 23: 685-698.
55. Martinez J, Huang X, Yang Y. Direct action of type I IFN on NK cells is required for their activation in response to vaccinia viral infection in vivo. *Journal of Immunology* 2008; 180: 1592-1597.
56. Swann JB, Hayakawa Y, Zerafa N, Sheehan KC, Scott B, Schreiber RD, Hertzog P, Smyth MJ. Type I IFN contributes to NK cell homeostasis, activation, and antitumor function. *Journal of Immunology* 2007; 178: 7540-7549.
57. Long EO, Kim HS, Liu D, Peterson ME, Rajagopalan S. Controlling natural killer cell responses: integration of signals for activation and inhibition. *Annual Review Immunology* 2013; 31: 227-258.

58. Madera S, Rapp M, Firth MA, Beilke JN, Lanier LL, Sun JC. Type I IFN promotes NK cell expansion during viral infection by protecting NK cells against fratricide. *Journal of Experimental Medicine* 2016; 213: 225-233.
59. Koivisto VA, Pelkonen R, Cantell K. Effect of interferon on glucose tolerance and insulin sensitivity. *Diabetes* 1989; 38: 641-647.
60. Campbell S, McLaren EH, Danesh BJ. Rapidly reversible increase in insulin requirement with interferon. *British Medical Journal* 1996; 313: 92.
61. Muraishi K, Sasaki Y, Kato T, Inada C, Tajiri Y, Yamada K. Classification and characteristics of interferon-related diabetes mellitus in Japan. *Hepatology Research*. 2011; 41: 184-188.
62. Honda K, Yanai H, Negishi H, Asagiri M, Sato M, Mizutani T, Shimada N, Ohba Y, Takaoka A, Yoshida N, Taniguchi T. IRF-7 is the master regulator of type-I interferon-dependent immune responses. *Nature* 2005; 434: 772-777.
63. Wang XA, Zhang R, Zhang S, Deng S, Jiang D, Zhong J, Yang L, Wang T, Hong S, Guo S, She ZG, Zhang XD, Li H. Interferon regulatory factor 7 deficiency prevents diet-induced obesity and insulin resistance. *American Journal of Physiology Endocrinology and Metabolism* 2013; 305: E485-495.
64. Parker B, Bruce I. SLE and metabolic syndrome. *Lupus* 2013; 22: 1259-1266.
65. Gyldenløve M, Storgaard H, Holst JJ, Vilsbøll T, Knop FK, Skov L. Patients with psoriasis are insulin resistant. *Journal of American Academy of Dermatology* 2015; 72: 599-605.
66. Mercer E, Rekedal L, Garg R, Lu B, Massarotti EM, Solomon DH. Hydroxychloroquine improves insulin sensitivity in obese non-diabetic individuals. *Arthritis Research & Therapy* 2012; 14: R135.

67. Wasko MC, McClure CK, Kelsey SF, Huber K, Orchard T, Toledo FG. 2015. Antidiabetogenic effects of hydroxychloroquine on insulin sensitivity and beta cell function: a randomised trial. *Diabetologia* 2015; 58: 2336-2343.
68. Macfarlane DE, Manzel L. Antagonism of immunostimulatory CpG-oligodeoxynucleotides by quinacrine, chloroquine, and structurally related compounds. *Journal of Immunology* 1998; 160: 1122-1131.
69. Kuznik A, Bencina M, Svajger U, Jeras M, Rozman B, Jerala R. Mechanism of endosomal TLR inhibition by antimalarial drugs and imidazoquinolines. *Journal of Immunology* 2011; 186: 4794-4804.
70. Franceschini L, Realdon S, Marcolongo M, Mirandola S, Bortoletto G, Alberti A. Reciprocal interference between insulin and interferon-alpha signaling in hepatic cells: a vicious circle of clinical significance? *Hepatology* 2011; 54: 484-494.
71. Merrill JT, Wallace DJ, Petri M, Kirou KA, Yao Y, White WI, Robbie G, Levin R, Berney SM, Chindalore V, Olsen N, Richman L, Le C, Jallal B, White B; Lupus Interferon Skin Activity (LISA) Study Investigators. Safety profile and clinical activity of sifalimumab, a fully human anti-interferon α monoclonal antibody, in systemic lupus erythematosus: a phase I, multicentre, double-blind randomised study. *Annals of Rheumatic Diseases* 2011; 70: 1905-1913.
72. Higgs BW, Zhu W, Morehouse C, White WI, Brohawn P, Guo X, Rebelatto M, Le C, Amato A, Greenberg SA, Drappa J, Richman L, Greth W, Jallal B, Yao Y. A phase 1b clinical trial evaluating sifalimumab, an anti-IFN α monoclonal antibody, shows target neutralisation of a type I IFN signature in blood of dermatomyositis and polymyositis patients. *Annals of Rheumatic Diseases* 2014; 73: 256-262.

FIGURE LEGENDS**Figure 1. VAT-derived chemerin recruits pDCs in obesity.**

(A) Chemerin ELISA was done on AEC-sups collected at different timepoints. Each dot represents AEC-sup generated from different VAT samples (N=14 at 36 hours). Comparisons among paired samples were done by paired T test (* $p < 0.05$).

(B) Migration of pDC (isolated from healthy donors) was assessed in response to AEC-sups in transwells. pDCs were either untreated or pretreated with anti-CMKLR1 or isotype control antibody and the number of migrated pDCs, were compared by performing two tailed paired T test ($p = 0.0185$). Cumulative data of six independent experiments (with different AEC-sup and pDC donor combinations) are represented.

(C) & (E) Total RNA was isolated from VAT of lean (N=11) and obese (N=83 individuals) and real-time PCR was done to determine the relative expression of CLEC4C and chemerin (TIG2) genes (normalized to the expression of 18S rRNA as reference gene). Expression of TIG2 (C) and CLEC4C (E) was compared between these two groups using Student's T test ($p = 0.8408$ for TIG2, $p = 0.004$ for CLEC4C).

(D) Plasma level of chemerin measured by ELISA was compared between lean and obese individuals using Student's T test ($p < 0.0001$).

(F) The relative expression values of TIG2 and CLEC4C in obese VAT were correlated based on Spearman's rank correlation (Spearman $r = 0.6203$, $p < 0.0001$).

(G) & (H) SVF was isolated from VAT samples by enzymatic digestion and were stained to enumerate frequency of pDCs ($CD45^+ CD3^- CD8^- CD123^+ CLEC4c^+$ cells) by flow cytometry and compared to pDC frequency (stained similarly) from peripheral blood of the same individuals. (G) a representative contour plot that was acquired by flow cytometry. (H) a scatter plot revealing relative enrichment of pDCs in VAT, as compared to peripheral blood

(N=15). Paired Student's T test (two tailed) was performed to show significant enrichment of pDCs in VAT ($p=.0071$).

(I) Representative images from immunofluorescence microscopy done on cryosections of VAT samples. Left panel shows merged image of a 200X field, nuclei are stained with DAPI (blue) and pDCs are stained with PE-labeled anti-BDCA4 antibody (red). Middle panel shows a digitally zoomed region showing DAPI staining and the right panel shows the merged image of the same zoomed region of the field. (BF = brightfield). Arrows shows BDCA4⁺ pDCs.

Figure 2. Type I interferon induction by VAT-recruited pDCs.

(A) Total RNA from VAT (N=83) collected from obese individuals was isolated and real time PCR was done for the pDC-specific transcript CLEC4C and four signature transcripts of type I IFN signaling (ISGs) viz. IRF7, TRIP14, MX1 and ISG15, relative expression was quantified taking 18S rRNA as reference gene. Interferon Signature Gene Index (ISGi) was formulated as the average of the relative expressions of the four selected ISGs in each sample. The relative expression values of CLEC4C were then related with ISGi values based on Spearman's rank correlation (Spearman $r = 0.4822$ $p < 0.0001$).

(B) Comparison of ISGi for VAT was compared between lean and obese individuals using Student's T test ($p < 0.0001$).

(C) AEC-sup was added to pDCs from healthy donors in increasing doses (25% and 75% total volume of culture media) and after overnight incubation supernatants were checked for presence of interferon- α (IFN α) by ELISA. Induction of IFN α by AEC-sup were validated by paired T test ($p = 0.0078$). Cumulative data of seven independent experiments (with different AEC-sup and pDC donor combinations) are represented.

(D) AEC-sups were treated with DNase (as described in experimental procedures) before addition to healthy pDC cultures. IFN α induction (measured by ELISA on the supernatants after overnight incubation) was compared with AEC-sup without any DNase treatment. Cumulative data of five independent experiments (with different AEC-sup and pDC donor combinations) are represented.

(E) AEC-sup (25% of total volume of 200 μ l in a well) were added to HEK-293 cells expressing TLR9 and reporting downstream NF κ B activation through secreted embryonic alkaline phosphatase (SEAP) reporter. Supernatants were collected after 12 hours and added to a SEAP substrate medium for further incubation. Optical density (OD) was then measured at 620nm on a spectrophotometer. Data from eight different AEC-sups are presented and compared with control medium-induced enzyme activity by unpaired T test ($p = 0.0062$).

(F) TLR9 gene expression was knocked down in pDCs isolated from healthy individuals using RNA interference. Knock down efficiency is presented in online supplemental figure 4A. Control (for EGFP) and target (for TLR9) siRNA transfected cells were cultured in presence of AEC-sup (75% of total volume of 100 μ l in a well) and after overnight incubation IFN α was measured in culture supernatants. Data from seven independent experiments are presented. Comparison between control and target-transfected cells were done by two tailed paired T test ($p=0.0024$).

Figure 3. HMGB1 aids activation of VAT-recruited plasmacytoid dendritic cells.

(A) AEC-sups (75% of total volume 100 μ l in a well) were added to healthy pDC culture and incubated overnight. In some conditions before addition of AEC-sups pDCs were treated with an anti-RAGE goat polyclonal antibody. ELISA was done to compare IFN α levels in

supernatants of anti-RAGE antibody treated or untreated pDCs. Cumulative data of seven independent experiments (with different AEC-sup and pDC donor combinations) are represented. Comparison between antibody-treated and untreated conditions was done by one tailed paired T test ($p=0.0078$).

(B) HMGB1 was depleted from AEC-sup using a monoclonal antibody and protein G magnetic beads. These AEC sups were then added (75% of total volume 100 μ l in a well) to pDC cultures and incubated overnight. ELISA was done for IFN α on the supernatants and comparison was done between HMGB1-depleted or control antibody-depleted AEC-sup treatments by unpaired T test ($p = 0.0482$).

(C) Total RNA from VAT N=79 was isolated and real time PCR was done for HMGB1 and the four ISGs viz. IRF7, TRIP14, MX1 and ISG15, relative expression was quantified taking 18S rRNA as reference gene. The relative expression values of CLEC4C were then related with ISGi values based on Spearman's rank correlation (Spearman $r = 0.2853$, $p = 0.0108$).

Figure 4: Proinflammatory macrophage polarization by type I interferons.

(A) – (D) CD14⁺ monocytes isolated from peripheral blood of healthy donors were developed into macrophages *in vitro* in presence of M-CSF and then into M2-type macrophages by adding recombinant human IL-4 in the culture. The cells were then further cultured in absence or presence of escalating doses of recombinant human IFN α . Then total RNA was isolated from the cells and real time PCR was done for two M2-signature genes, F13A1 (A) and CCL22 (B), as well as two M1-signature genes, IRF5 (C) and NOS2 (D). In presence of IFN α , the M2-polarized cells showed reduction in the M2-signature genes and induction of the M1-signature

genes. Statistical significance was checked by paired T test. Cumulative data of three to seven independent experiments are represented.

(E) & (F) Macrophages generated as described in (A)-(D) were assessed for surface expression of the M2 specific marker CD206 and the M1-specific marker CD86 by flow cytometry. (E) shows histograms of a representative experiment for both the markers and (F) shows cumulative data of mean fluorescence intensity from five independent experiments. Statistical significance was checked by two tailed paired T test.

(G) Enzyme linked immunosorbent assay was done for TNF α on supernatants collected at the end of the culture from the macrophages generated as described above, absorbance was taken at 450nm ($p=0.0313$, Wilcoxon matched pairs signed rank test).

Figure 5: Role of plasmacytoid dendritic cells and type I IFNs in proinflammatory polarization of macrophages in the context of metaflammation

(A) – (C) *In vitro* generated M2 macrophages were cultured with AEC-sup (75% of total volume 200 μ l in a well) in presence or absence of autologous pDCs (A). After two days cells were harvested and used for flow cytometric assessment of M2-specific surface marker CD206 (B) and M1-specific surface marker CD86 (C) on CD11b⁺ macrophages.

(D) Culture supernatants from the co-culture experiment described in (A) were harvested and IFN α was measured by ELISA, comparison done by paired T test, ($p=0.0131$).

(E) SVF was isolated from VAT samples by enzymatic digestion and were stained to isolate M1-type (CD45⁺ CD11b⁺ CD11c⁺ cells) and M2-type (CD45⁺ CD11b⁺ CD163⁺ cells) by flow cytometry; a representative contour plot is shown.

(F) – (G) Total RNA was isolated from the sorted M1-type and M2-type cells and expression data from qPCR for two M1-signature genes, IRF5 (F) and NOS2 (G) are compared between two subsets (N=7).

(H) ISGi (calculated as average of expression of four ISGs viz. IRF7, TRIP14, MX1 and ISG15 as before) is compared between M2 and M1 macrophages (N=7).

(I) – (J) Relative expression of ISGs (ISGi) was correlated with relative expression of IRF5 and NOS2 in the sorted CD11c⁺ M1 macrophages based on Spearman's rank correlation (IRF5 vs ISGi: N=7, Spearman r = 0.9286, p = 0.0022; NOS2 vs ISGi: N=6, Spearman r = 0.8857, p = 0.0333).

Figure 6: Relating tissue type I IFN response to macrophage composition.

(A) & (B) Correlation of VAT expression of IRF5 (A) with tissue ISGi (N=82, Spearman r = 0.4736 , p < 0.0001) and with VAT expression of the signature pDC transcript CLEC4C (N=82, Spearman r = 0.4962 , p < 0.0001) is represented.

(C) Ratio of M1 (CD11c⁺) to M2 (CD163⁺) macrophage frequency (% of CD45⁺ CD11b⁺ cells) in VAT was related with whole tissue ISGi based on Spearman's rank correlation (N=11; Spearman r = 0.5909, p =0.0278).

Figure 7: Relationship between VAT type I IFN induction with insulin resistance and the proposed model for role of pDCs in metaflammation.

(A) – (C) Insulin resistance in adipose tissue was assessed using ADIPO-IR index as described, calculated from circulating free fatty acid and insulin levels and the relationship between VAT ISGi and corresponding ADIPO-IR values are represented. Two distinct groups, one with a left-

shifted correlation (designated group L) and another with a right-shifted correlation (designated group R) are demarcated with the red broken line in (A). The same correlation in the individual groups are shown in (B) and (C).

(D) & (E) HOMA2-IR was calculated using levels of fasting blood glucose and insulin as described. Relationship between VAT ISGi and corresponding HOMA2-IR values are represented for group L in (D) (Spearman $r = 0.6377$, $p = 0.0003$) and for group R in (E) (Spearman $r = 0.5103$, $p = 0.0017$).

(F) Relationship between VAT ISGi and corresponding HbA1C values are represented for group R (Spearman $r = 0.4273$, $p = 0.0233$).

(G) The model based on our data proposes that visceral adipose tissue (VAT)-derived chemerin recruits circulating plasmacytoid dendritic cells (pDCs) through the CMKLR1 receptor. VAT-recruited pDCs are activated *in situ* by HMGB1-nucleic acid complexes that may access Toll-like receptor-9 (TLR9) in pDCs via RAGE receptors. PDCs thus activated produce type I IFNs *in situ*, which in turn can fuel *in situ* polarization of M2 macrophages to proinflammatory M1 macrophages expressing IRF5. The proinflammatory M1 macrophages in turn contribute to propagation of chronic inflammation in VAT and insulin resistance.

Table 1: Anthropometric and biochemical parameters of the recruited individuals.

Parameters	Data available (N)		Values	
	Obese	Lean	Obese	Lean
Total	83	29	-	-
Female	49	8	-	-
Male	34	21	-	-
Age, years	83	29	41.2857(±12.0866)	44.7241(±11.4483)
Body mass index	76	29	43.9388(±7.46692)	25.07037(±3.09401)
VAT samples	83	11	-	-
Plasma samples	72	28	-	-
Fasting blood glucose, mg/dl	78	29	128.7462(±59.1401)	103.5862 (±19.4082)
Fasting plasma insulin, µU/ml	63	0	25.3906(±14.2685)	Not available
Glycated hemoglobin 1c, % (NGSP)	63	20	7.15873(±1.719118)	5.445 (± 0.551052)
Glycated hemoglobin 1c, mmol/mol (IFCC)	63	20	57.23809(±21.8216)	35.9(± 6.086223)
Plasma free fatty acid (µM)	64	0	296.6826 (±114.731)	Not available
Plasma chemerin (ng/ml)	72	28	75.2466 (±23.2116)	15.4 (±18.6437)
ADIPO-IR	64	0	49.198 (±37.125)	Not available
HOMA2-IR	63	0	3.5211(±2.0888)	Not available

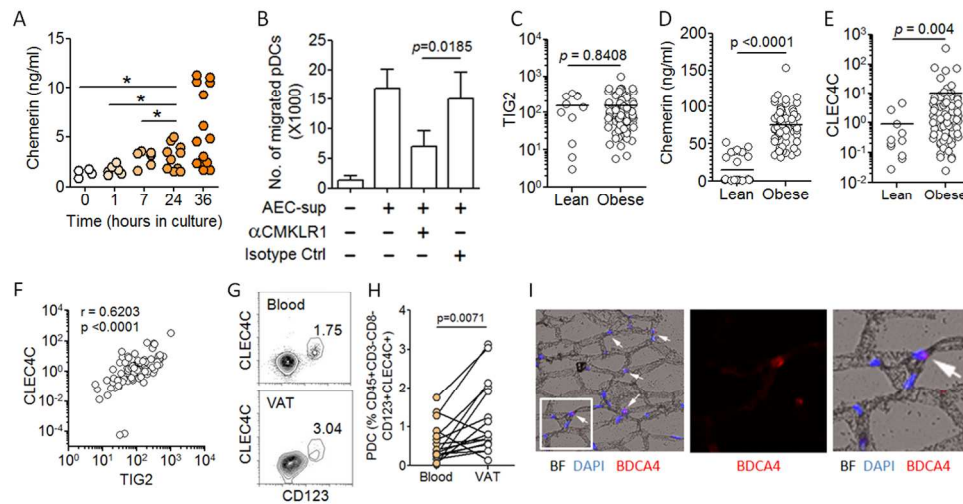


Figure 1

Figure 1. VAT-derived chemerin recruits pDCs in obesity. (A) Chemerin ELISA was done on AEC-sups collected at different timepoints. Each dot represents AEC-sup generated from different VAT samples (N=14 at 36 hours). Comparisons among paired samples were done by paired T test (* $p < 0.05$). (B) Migration of pDC (isolated from healthy donors) was assessed in response to AEC-sups in transwells. pDCs were either untreated or pretreated with anti-CMKLR1 or isotype control antibody and the number of migrated pDCs, were compared by performing two tailed paired T test ($p = 0.0185$). Cumulative data of six independent experiments (with different AEC-sup and pDC donor combinations) are represented. (C) & (E) Total RNA was isolated from VAT of lean (N=11) and obese (N=83 individuals) and real-time PCR was done to determine the relative expression of CLEC4C and chemerin (TIG2) genes (normalized to the expression of 18S rRNA as reference gene). Expression of TIG2 (C) and CLEC4C (E) was compared between these two groups using Student's T test ($p = 0.8408$ for TIG2, $p = 0.004$ for CLEC4C). (D) Plasma level of chemerin measured by ELISA was compared between lean and obese individuals using Student's T test ($p < 0.0001$). (F) The relative expression values of TIG2 and CLEC4C in obese VAT were correlated based on Spearman's rank correlation (Spearman $r = 0.6203$, $p < 0.0001$). (G) & (H) SVF was isolated from VAT samples by enzymatic digestion and were stained to enumerate frequency of pDCs (CD45⁺ CD3⁻ CD8⁻ CD123⁺ CLEC4c⁺ cells) by flow cytometry and compared to pDC frequency (stained similarly) from peripheral blood of the same individuals. (G) a representative contour plot that was acquired by flow cytometry. (H) a scatter plot revealing relative enrichment of pDCs in VAT, as compared to peripheral blood (N=15). Paired Student's T test (two tailed) was performed to show significant enrichment of pDCs in VAT ($p = .0071$). (I) Representative images from immunofluorescence microscopy done on cryosections of VAT samples. Left panel shows merged image of a 200X field, nuclei are stained with DAPI (blue) and pDCs are stained with PE-labeled anti-BDCA4 antibody (red). Middle panel shows a digitally zoomed region showing DAPI staining and the right panel shows the merged image of the same zoomed region of the field. (BF = brightfield). Arrows shows BDCA4⁺ pDCs.

180x106mm (300 x 300 DPI)

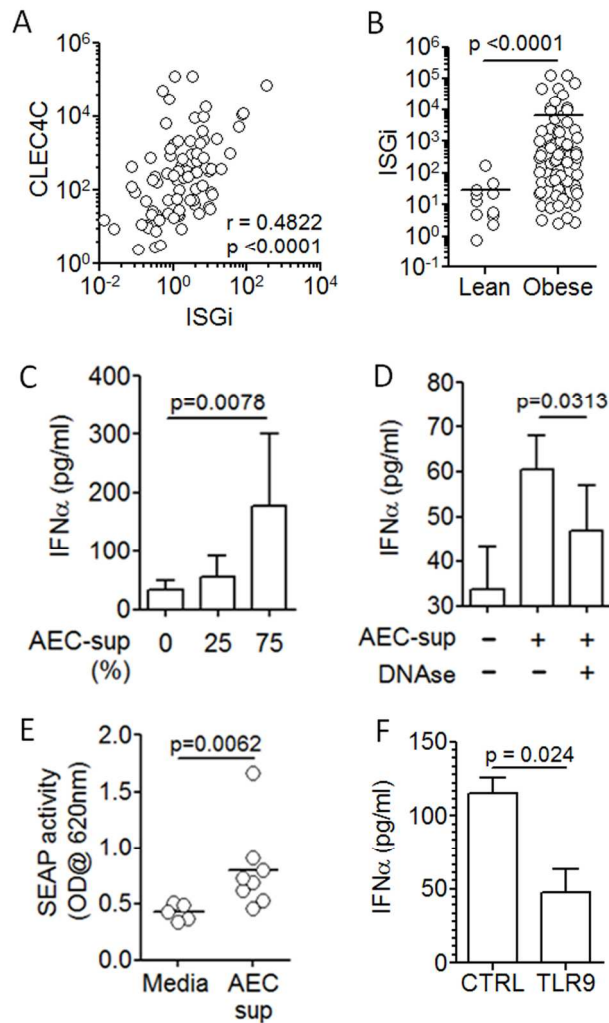


Figure 2

Figure 2. Type I interferon induction by VAT-recruited pDCs. (A) Total RNA from VAT (N=83) collected from obese individuals was isolated and real time PCR was done for the pDC-specific transcript CLEC4C and four signature transcripts of type I IFN signaling (ISGs) viz. IRF7, TRIP14, MX1 and ISG15, relative expression was quantified taking 18S rRNA as reference gene. Interferon Signature Gene Index (ISGi) was formulated as the average of the relative expressions of the four selected ISGs in each sample. The relative expression values of CLEC4C were then related with ISGi values based on Spearman's rank correlation (Spearman $r = 0.4822$ $p < 0.0001$). (B) Comparison of ISGi for VAT was compared between lean and obese individuals using Student's T test ($p < 0.0001$). (C) AEC-sup was added to pDCs from healthy donors in increasing doses (25% and 75% total volume of culture media) and after overnight incubation supernatants were checked for presence of interferon- α (IFN α) by ELISA. Induction of IFN α by AEC-sups were validated by paired T test ($p = 0.0078$). Cumulative data of seven independent experiments (with different AEC-sup and pDC donor combinations) are represented. (D) AEC-sups were treated with DNase (as described in experimental procedures) before addition to healthy pDC cultures. IFN α induction (measured by ELISA on

the supernatants after overnight incubation) was compared with AEC-sup without any DNase treatment. Cumulative data of five independent experiments (with different AEC-sup and pDC donor combinations) are represented. (E) AEC-sup (25% of total volume of 200 μ l in a well) were added to HEK-293 cells expressing TLR9 and reporting downstream NF κ B activation through secreted embryonic alkaline phosphatase (SEAP) reporter. Supernatants were collected after 12 hours and added to a SEAP substrate medium for further incubation. Optical density (OD) was then measured at 620nm on a spectrophotometer. Data from eight different AEC-sup are presented and compared with control medium-induced enzyme activity by unpaired T test ($p = 0.0062$). (F) TLR9 gene expression was knocked down in pDCs isolated from healthy individuals using RNA interference. Knock down efficiency is presented in online supplemental figure 4A. Control (for EGFP) and target (for TLR9) siRNA transfected cells were cultured in presence of AEC-sup (75% of total volume of 100 μ l in a well) and after overnight incubation IFN α was measured in culture supernatants. Data from seven independent experiments are presented. Comparison between control and target-transfected cells were done by two tailed paired T test ($p=0.0024$).

88x157mm (300 x 300 DPI)

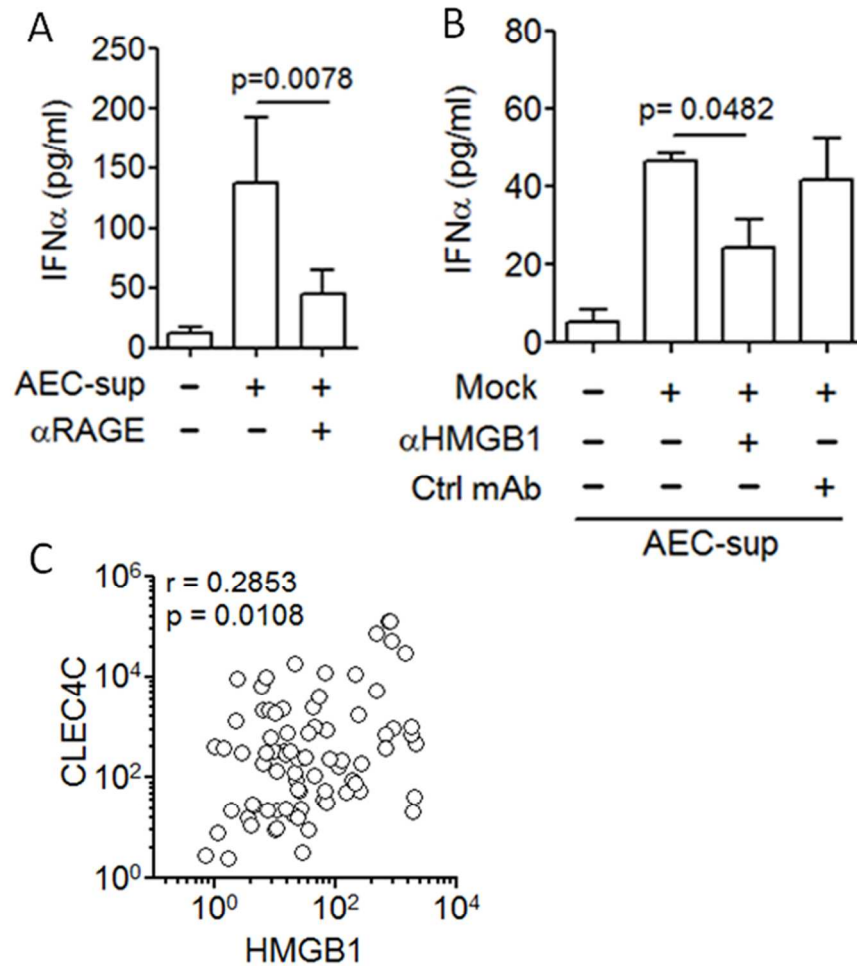


Figure 3

Figure 3. HMGB1 aids activation of VAT-recruited plasmacytoid dendritic cells. (A) AEC-sups (75% of total volume 100 μ l in a well) were added to healthy pDC culture and incubated overnight. In some conditions before addition of AEC-sups pDCs were treated with an anti-RAGE goat polyclonal antibody. ELISA was done to compare IFN α levels in supernatants of anti-RAGE antibody treated or untreated pDCs. Cumulative data of seven independent experiments (with different AEC-sup and pDC donor combinations) are represented.

Comparison between antibody-treated and untreated conditions was done by one tailed paired T test ($p=0.0078$). (B) HMGB1 was depleted from AEC-sups using a monoclonal antibody and protein G magnetic beads. These AEC sups were then added (75% of total volume 100 μ l in a well) to pDC cultures and incubated overnight. ELISA was done for IFN α on the supernatants and comparison was done between HMGB1-depleted or control antibody-depleted AEC-sup treatments by unpaired T test ($p = 0.0482$). (C) Total RNA from VAT N=79 was isolated and real time PCR was done for HMGB1 and the four ISGs viz. IRF7, TRIP14, MX1 and ISG15, relative expression was quantified taking 18S rRNA as reference gene. The relative expression values of CLEC4C were then related with ISGI values based on Spearman's rank correlation

(Spearman $r = 0.2853$, $p = 0.0108$).

88x110mm (300 x 300 DPI)

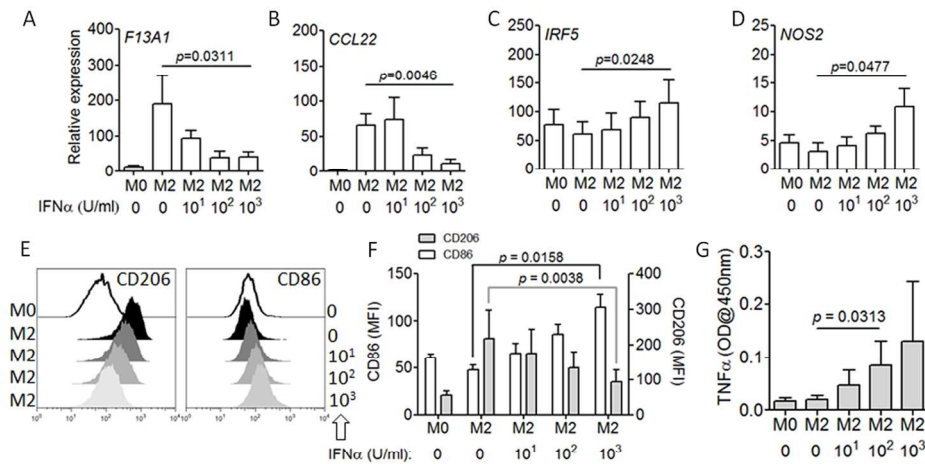


Figure 4

Figure 4: Proinflammatory macrophage polarization by type I interferons. (A) – (D) CD14⁺ monocytes isolated from peripheral blood of healthy donors were developed into macrophages in vitro in presence of M-CSF and then into M2-type macrophages by adding recombinant human IL-4 in the culture. The cells were then further cultured in absence or presence of escalating doses of recombinant human IFN α . Then total RNA was isolated from the cells and real time PCR was done for two M2-signature genes, F13A1 (A) and CCL22 (B), as well as two M1-signature genes, IRF5 (C) and NOS2 (D). In presence of IFN α , the M2-polarized cells showed reduction in the M2-signature genes and induction of the M1-signature genes. Statistical significance was checked by paired T test. Cumulative data of three to seven independent experiments are represented. (E) & (F) Macrophages generated as described in (A)-(D) were assessed for surface expression of the M2 specific marker CD206 and the M1-specific marker CD86 by flow cytometry. (E) shows histograms of a representative experiment for both the markers and (F) shows cumulative data of mean fluorescence intensity from five independent experiments. Statistical significance was checked by two tailed paired T test. (G) Enzyme linked immunosorbent assay was done for TNF α on supernatants collected at the end of the culture from the macrophages generated as described above, absorbance was taken at 450nm (p=0.0313, Wilcoxon matched pairs signed rank test).

180x102mm (300 x 300 DPI)

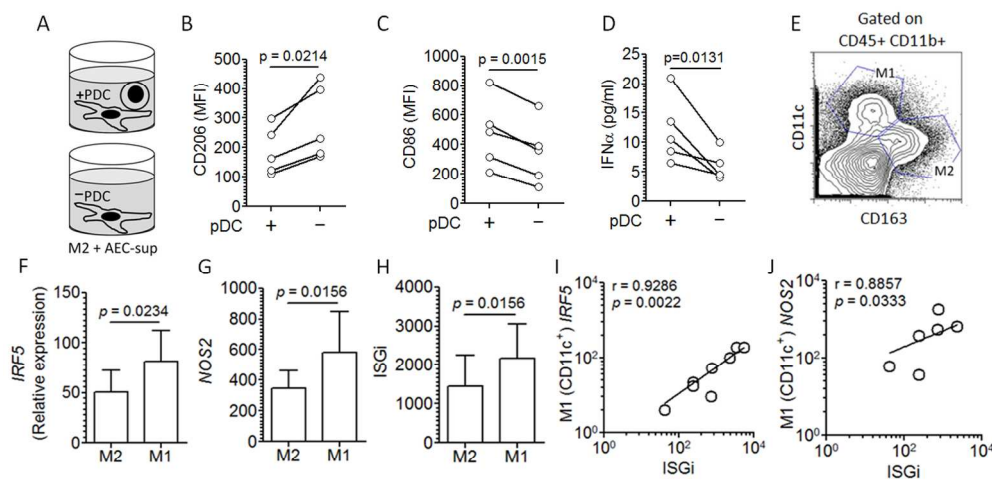


Figure 5

Figure 5: Role of plasmacytoid dendritic cells and type I IFNs in proinflammatory polarization of macrophages in the context of metaflammation (A) – (C) In vitro generated M2 macrophages were cultured with AEC-sup (75% of total volume 200 μ l in a well) in presence or absence of autologous pDCs (A). After two days cells were harvested and used for flow cytometric assessment of M2-specific surface marker CD206 (B) and M1-specific surface marker CD86 (C) on CD11b⁺ macrophages. (D) Culture supernatants from the co-culture experiment described in (A) were harvested and IFN α was measured by ELISA, comparison done by paired T test, ($p=0.0131$). (E) SVF was isolated from VAT samples by enzymatic digestion and were stained to isolate M1-type (CD45⁺ CD11b⁺ CD11c⁺ cells) and M2-type (CD45⁺ CD11b⁺ CD163⁺ cells) by flow cytometry; a representative contour plot is shown. (F) – (G) Total RNA was isolated from the sorted M1-type and M2-type cells and expression data from qPCR for two M1-signature genes, IRF5 (F) and NOS2 (G) are compared between two subsets (N=7). (H) ISGi (calculated as average of expression of four ISGs viz. IRF7, TRIP14, MX1 and ISG15 as before) is compared between M2 and M1 macrophages (N=7). (I) – (J) Relative expression of ISGs (ISGi) was correlated with relative expression of IRF5 and NOS2 in the sorted CD11c⁺ M1 macrophages based on Spearman's rank correlation (IRF5 vs ISGi: N=7, Spearman $r = 0.9286$, $p = 0.0022$; NOS2 vs ISGi: N=6, Spearman $r = 0.8857$, $p = 0.0333$).

180x101mm (300 x 300 DPI)

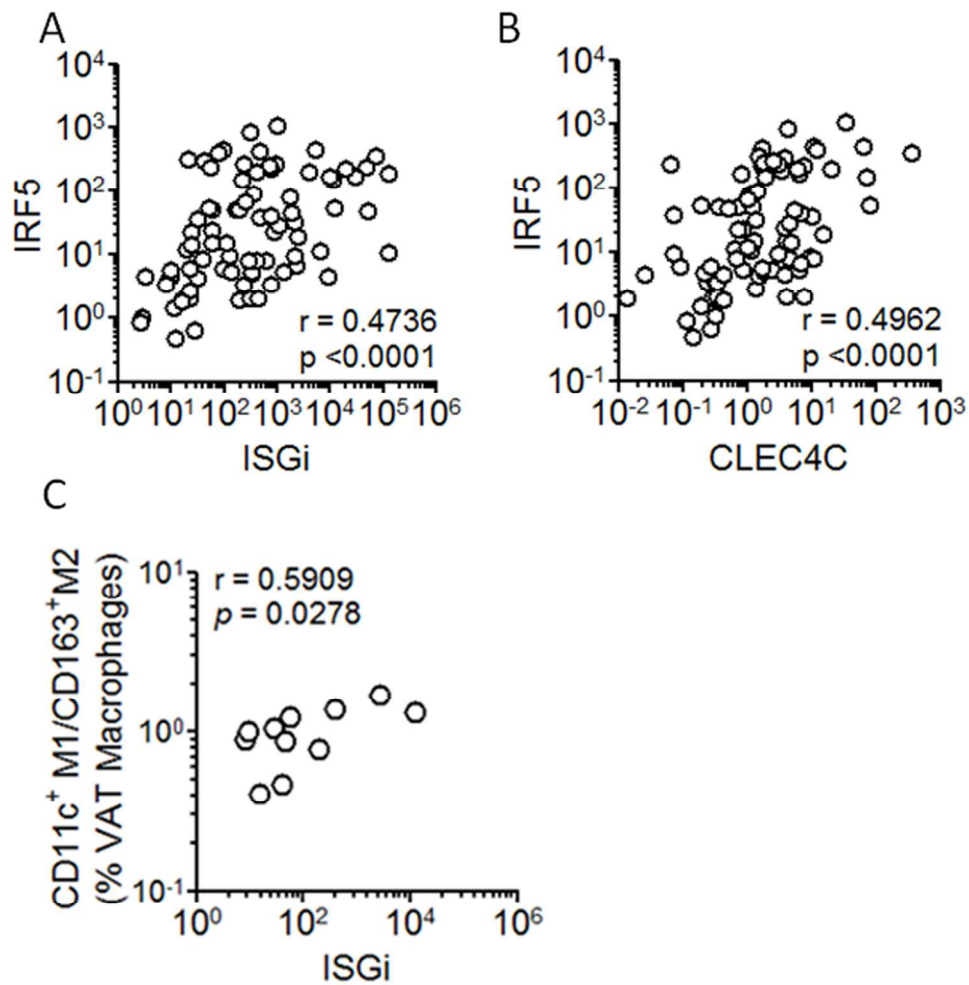


Figure 6

Figure 6: Relating tissue type I IFN response to macrophage composition. (A) & (B) Correlation of VAT expression of IRF5 (A) with tissue ISGi (N=82, Spearman $r = 0.4736$, $p < 0.0001$) and with VAT expression of the signature pDC transcript CLEC4C (N=82, Spearman $r = 0.4962$, $p < 0.0001$) is represented. (C) Ratio of M1 (CD11c+) to M2 (CD163+) macrophage frequency (% of CD45+ CD11b+ cells) in VAT was related with whole tissue ISGi based on Spearman's rank correlation (N=11; Spearman $r = 0.5909$, $p = 0.0278$).

88x99mm (300 x 300 DPI)

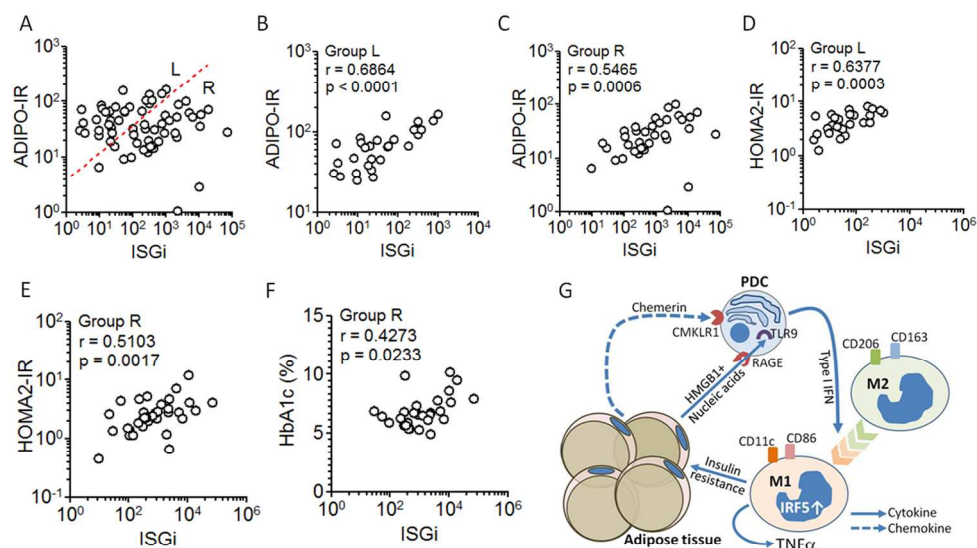


Figure 7

Figure 7: Relationship between VAT type I IFN induction with insulin resistance and the proposed model for role of pDCs in metaflammation. (A) – (C) Insulin resistance in adipose tissue was assessed using ADIPO-IR index as described, calculated from circulating free fatty acid and insulin levels and the relationship between VAT ISGi and corresponding ADIPO-IR values are represented. Two distinct groups, one with a left-shifted correlation (designated group L) and another with a right-shifted correlation (designated group R) are demarcated with the red broken line in (A). The same correlation in the individual groups are shown in (B) and (C). (D) & (E) HOMA2-IR was calculated using levels of fasting blood glucose and insulin as described. Relationship between VAT ISGi and corresponding HOMA2-IR values are represented for group L in (D) (Spearman $r = 0.6377$, $p = 0.0003$) and for group R in (E) (Spearman $r = 0.5103$, $p = 0.0017$). (F) Relationship between VAT ISGi and corresponding HbA1c values are represented for group R (Spearman $r = 0.4273$, $p = 0.0233$). (G) The model based on our data proposes that visceral adipose tissue (VAT)-derived chemerin recruits circulating plasmacytoid dendritic cells (pDCs) through the CMKLR1 receptor. VAT-recruited pDCs are activated in situ by HMGB1-nucleic acid complexes that may access Toll-like receptor-9 (TLR9) in pDCs via RAGE receptors. pDCs thus activated produce type I IFNs in situ, which in turn can fuel in situ polarization of M2 macrophages to proinflammatory M1 macrophages expressing IRF5. The proinflammatory M1 macrophages in turn contribute to propagation of chronic inflammation in VAT and insulin resistance.

180x116mm (300 x 300 DPI)

Online supplemental materials

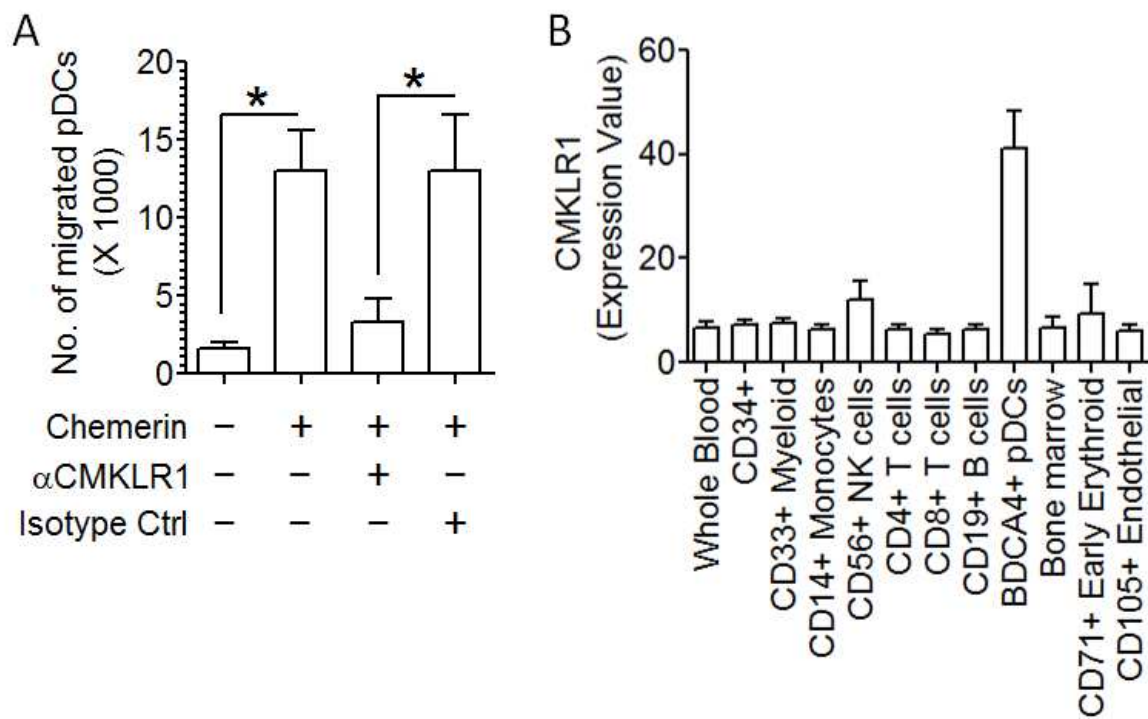
For manuscript:

‘Adipose recruitment and activation of plasmacytoid dendritic cells fuel metaflammation’

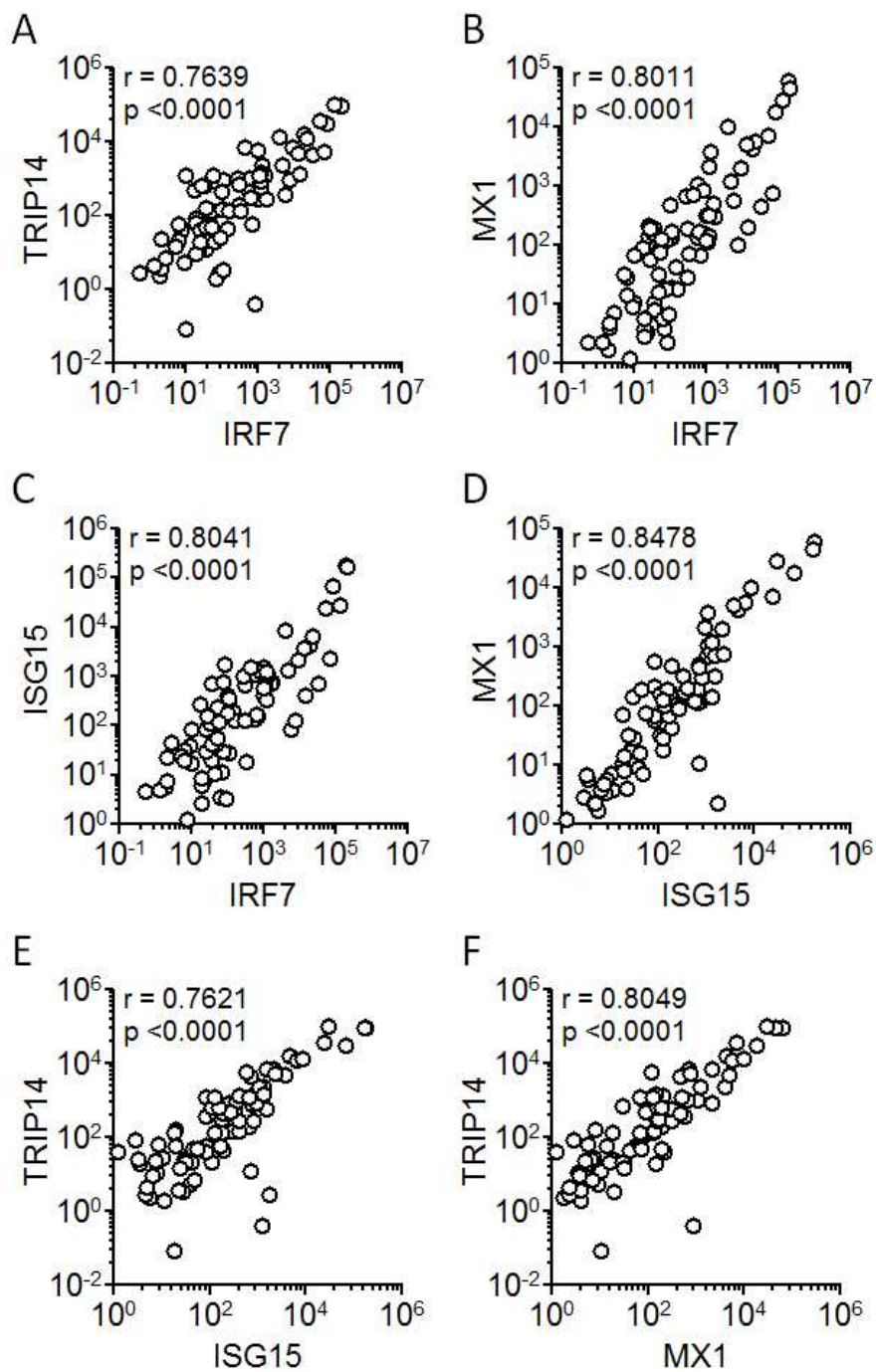
Amrit Raj Ghosh et al.

Online Supplemental Table S1: Primer oligonucleotide sequences used in real time PCR

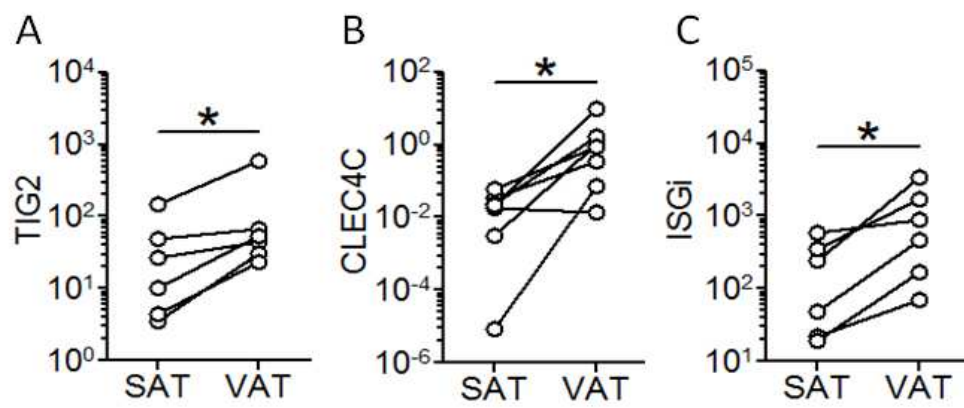
GENES	PRIMER	SEQUENCE
<i>IRF7</i>	FORWARD	ACCTGTAGCCCCCTCTGCCA
	REVERSE	GTGGGGCTGCCCTCTCAGGA
<i>TRIP14</i>	FORWARD	GAGCCCTGGGGCCTTCTCTTC
	REVERSE	GCTCTGGGGGACCTGGCTTTC
<i>MX1</i>	FORWARD	ACTCCTCTGGGAGGGTGGCT
	REVERSE	GCACCTCCTTGGGAATGGTGGCT
<i>ISG15</i>	FORWARD	CTACGAGGTCCGGCTGACGC
	REVERSE	GTGGAGGCCCTTAGCTCCGC
<i>TIG2</i>	FORWARD	TGAGGAGCACCAGGAGAC
	REVERSE	TTGGAGAAGGCCGAACTGTC
<i>CLEC4C</i>	FORWARD	GACCGAGAGAAAGGACTCTGGTGG
	REVERSE	AGTCCAAGGGGTTGGGCAGC
<i>HMGB1</i>	FORWARD	ACATCCAAAATCTTGATCAGTTA
	REVERSE	AGGACAGACTTTCAAATGTTT
<i>IRF5</i>	FORWARD	CGGACTGATGTGGAGATGTG
	REVERSE	CTCTCCTTCTTGGCCCAAAT
<i>CCL22</i>	FORWARD	GCAACTGAGGCAGGCCCTA
	REVERSE	CCTGGAGGAGCCAAGGCCAC
<i>NOS2</i>	FORWARD	AGCTCAACAACAAATTCAGG
	REVERSE	ATCAATGTCATGAGCAAAGG
<i>F13A1</i>	FORWARD	GAGCGCCTGCAGGACCTTGT
	REVERSE	GCCCTCTGCGGACAATCAGC
<i>TLR9</i>	FORWARD	AAATCCCTCATATCCCTGTC
	REVERSE	TTGTAATAACAGTTGCCGTC
<i>I8S</i>	FORWARD	GTAACCCGTTGAACCCATT
	REVERSE	CCATCCAATCGGTAGTAGCG



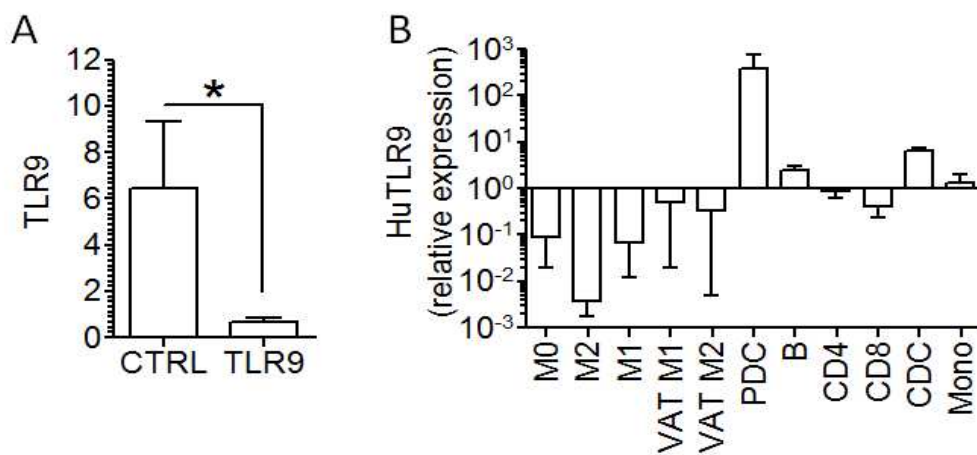
Online Supplemental Figure 1



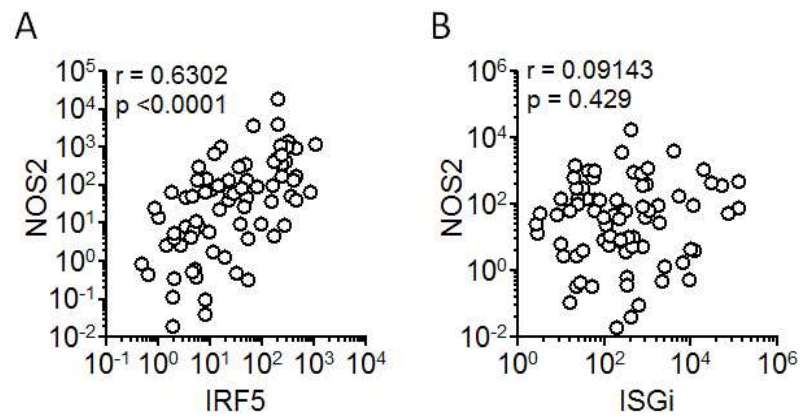
Online Supplemental Figure 2



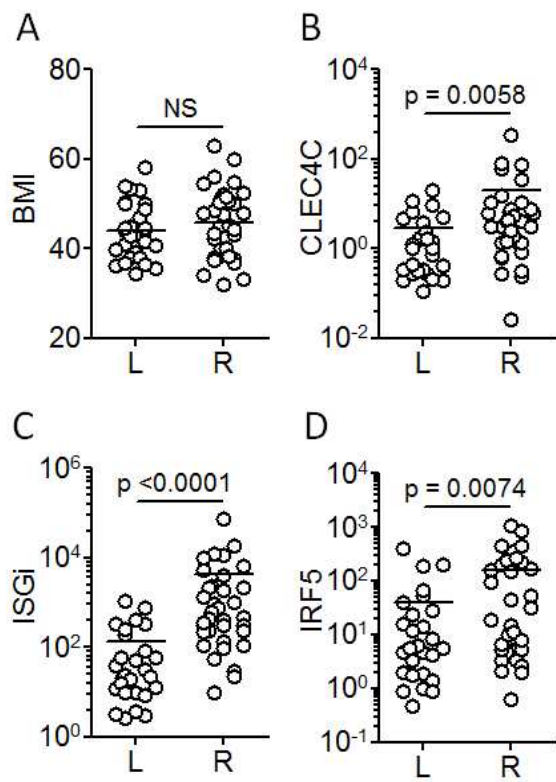
Online Supplemental Figure 3



Online Supplemental Figure 4



Online Supplemental Figure 5



Online Supplemental Figure 6

Online Supplemental Figure 1: Function and restricted expression of chemerin receptor CMKLR1 plasmacytoid dendritic cells.

(A) Migration of pDC was assessed in response to human recombinant chemerin in transwells. pDCs were either untreated or pretreated with anti-CMKLR1 or isotype control antibody and the number of migrated pDCs, were compared by performing two tailed paired T test (* $p < 0.05$). Cumulative data of three independent experiments are represented.

(B) Expression data of CMKLR1 on different human immune cell subsets collated from high density oligonucleotide array database GSE1133 (accessed from <http://ds.bioGPS.org/?dataset=GSE1133&gene=1240>), showing restricted expression on plasmacytoid dendritic cells. Normalized expression data (mean \pm SD) are presented for two different probes targeting CMKLR1 (207652_s_at and 210659_at) each in duplicate.

Online Supplemental Figure 2: Coherent expression of the selected type I IFN signature genes in VAT.

(A)-(F) Coherent expression of the four interferon signature genes or ISGs (*IRF7*, *TRIP14*, *MX1* and *ISG15*) in VAT, validating their selection to formulate the interferon signature gene index (ISGi). Correlation of expression was checked with Spearman's ranked correlation (N=83).

Online Supplemental Figure 3: Comparison of gene expression between subcutaneous and visceral adipose tissue samples.

(A)-(C) Paired samples of subcutaneous adipose tissue (SAT) with VAT samples (N=6) were assessed for expression of TIG2, enrichment of CLEC4C transcript and value of interferon signature gene index. Comparisons were done by performing two tailed paired T test (* $p < 0.05$).

Online Supplemental Figure 4: TLR9 knock down in pDCs and expression of TLR9 in different immune cell subsets.

(A) TLR9 expression was knocked down in pDCs using siRNA transfection. Comparison between control and target siRNA transfection was done by paired T test (* $p < 0.05$).

(B) Expression of TLR9 was assessed by real time PCR in circulating plasmacytoid DCs (pDC), B cells (B), CD4 T cells (CD4), CD8 T cells (CD8), conventional dendritic cells (cDC), monocytes (Mono), *in vitro* generated M1 and M2 macrophages (M1 and M2) and *ex vivo* isolated M1 and M2 macrophages from visceral adipose tissue of obese individuals (Vat M1 and Vat M2).

Online Supplemental Figure 5: Coherent expression of the genes selected as signature for M1 macrophages.

(A) Coherent expression of the genes *IRF5* and *NOS2* in VAT. Correlation of expression was checked with Spearman's ranked correlation (N=79, $r = 0.6302$, $p < 0.0001$).

(B) Relationship between VAT expression of *NOS2* and tissue ISGi (N=77, $r = 0.99143$, $p = 0.429$).

Online Supplemental Figure 6: Comparison of group L and group R with respect to body mass index and gene expression

(A) Comparison of body mass index between group L and group R (NS= not significant).

(B)-(D) Comparison between group L and group R for expression of pDC-specific transcript CLEC4C (B), interferon signature gene index (C) and expression of M1 macrophage signature IRF5 (D)